AD-A083 652 SKF INDUSTRIES INC KING OF PRUSSIA PA F/G 1/3
SMALL PORTABLE ANALYZER DIAGNOSTIC EQUIPMENT (SPADE) - ADVANCE --ETC(U)
SEP 79 D B BOARD DAAJ01-76-C-1073
UNCLASSIFIED SKF-AL99Q016 USAAVRADCOM-TR-80-F-3 NL

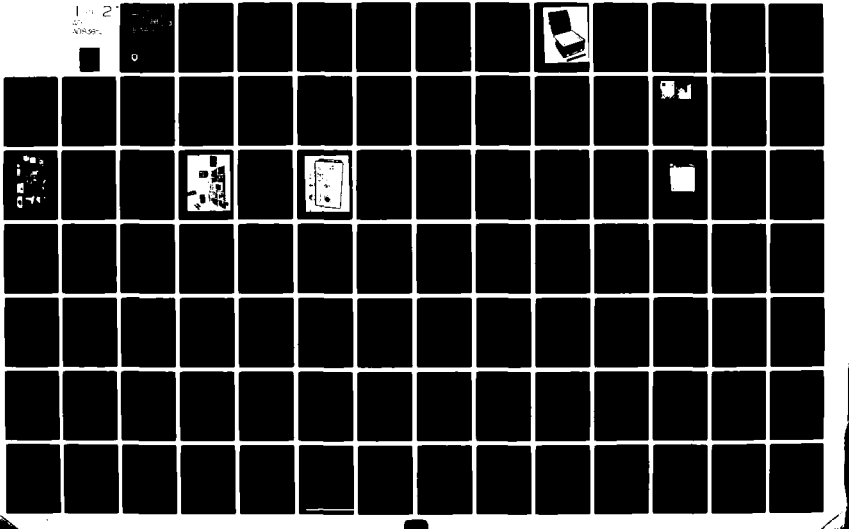

12

AVRADCOM

Technical Report TR 80-F-3

AD

LEVEL II

DTIC ELECTE APR 28 1980 S D

E

AD A083652

SMALL PORTABLE ANALYZER DIAGNOSTIC EQUIPMENT (SPADE)

ADVANCE DEVELOPMENT PROTOTYPE REPORT

SKF INDUSTRIES INC.
DAVID B. BOARD

SEPTEMBER, 1979

Approved for public release; distribution unlimited.

DDC FILE COPY

80 4 28 092

UNCLASSIFIED

SECURITY CLASSIFICATION OF THIS PAGE (When Data Entered)

REPORT DOCUMENTATION PAGE	READ INSTRUCTIONS BEFORE COMPLETING FORM
1. REPORT NUMBER AVRADCOM Technical Report TR 80-F-3	2. GOVT ACCESSION NO. AD-A083652	3. RECIPIENT'S CATALOG NUMBER
4. TITLE (and Subtitle) Small Portable Analyzer Diagnostic Equipment (SPADE) - Advance Development Prototype Report		5. TYPE OF REPORT & PERIOD COVERED Final Report
		6. PERFORMING ORG. REPORT NUMBER SKF Report AL79Q016
7. AUTHOR(s) David B. Board		8. CONTRACT OR GRANT NUMBER(s) DAAJ01-76-C-1073 (PGC)
9. PERFORMING ORGANIZATION NAME AND ADDRESS SKF Indistries Inc 1100 1st Ave King of Prussia PA 19406		10. PROGRAM ELEMENT, PROJECT, TASK AREA & WORK UNIT NUMBERS
11. CONTROLLING OFFICE NAME AND ADDRESS Directorate for Systems Engineering US Army Aivation R&D Command PO Box 209 St. Louis MO 63166		12. REPORT DATE Sep 1979 13. NUMBER OF PAGES 110
14. MONITORING AGENCY NAME & ADDRESS(if different from Controlling Office) USAAVRADCOM TR 80-F-3		15. SECURITY CLASS. (of this report) UNCLAS 15a. DECLASSIFICATION/DOWNGRADING SCHEDULE

16. DISTRIBUTION STATEMENT (of this Report)

Approved for public release, distribution unlimited

SKF-AL79Q016

17. DISTRIBUTION STATEMENT (of the abstract entered in Block 20, if different from Report)

18. SUPPLEMENTARY NOTES

19. KEY WORDS (Continue on reverse side if necessary and identify by block number)

diagnostic equipment
helicopter
bearings
shock pulse technique

20. ABSTRACT (Continue on reverse side if necessary and identify by block number)

This report documents the contractors SKF Industries Inc design development and field evaluation of the Small Portable Analyzer Diagnostic Equipment (SPADE). The SPADE is an advanced development prototype of an off board aircraft bearing diagnostic equipment. The SPADE works on the shock pulse principle, which measures the kinetic impact and frictional energy within the tested component, independent of background vibration. The SPADE provides a highly accurate and trendable measurement of bearing condition that is

DD FORM 1 JAN 73 1473 EDITION OF 1 NOV 65 IS OBSOLETE

SECURITY CLASSIFICATION OF THIS PAGE (When Data Entered)

20.. Abstract

independent of non-defect related background vibrations caused by the elastic motions of structures, rotors, gears, and shafts. The SPADE employs specialized signal conditioning and data processing techniques to measure frictional and shock energy associated with abrasive wear and dynamic impact of contaminated, pitted, spalled, corroded, or brinnelled bearing contact surfaces. This measured energy is then compared to present limits (stored in SPADE memory) that are representative of good, marginal, and discrepant conditions, and the status of the monitored component is displayed on the instrument's control panel. The unit has sufficient internal memory capacity to automatically process data from up to twenty-two (22) sensor locations on each of eight different aircraft models. It provides component condition readout in the form of a green (good), yellow (caution), or red (remove) light and a two digit percent degradation display to allow trending of discrepent component in the yellow (caution) zone. It is designed and packaged to survive the army field maintenance environment and can be operated by semi-skilled personnel.

SMALL PORTABLE ANALYZER
DIAGNOSTIC EQUIPMENT
(SPADE)

FINAL REPORT

SEPTEMBER 1979

PREPARED BY: DAVID B. BOARD

U. S. ARMY CONTRACT NO. DAAJ01-76-C-1973 (P6C)

SUBMITTED TO:

DEPARTMENT OF THE ARMY

U. S. ARMY AVIATION RESEARCH AND DEVELOPMENT COMMAND

P. O. Box 209

ST. LOUIS, MO. 63166

SKF REPORT AL79Q016

SKF CODE LC415

CONTENTS

SECTION		PAGE
1.0	Abstract	1
2.0	Executive Summary	2
2.1	Background	2
2.2	Technical Approach	2
2.3	Program Synopsis	4
2.4	SPADE Diagnostic Accuracy	6
2.5	Conclusions & Recommendations	7
3.0	SPADE Design, Development, & Lab Test	13
3.1	Shock Pulse Analysis	13
3.2	SPADE Hardware Design & Development	23
3.3	SPADE Field Test Prototype Functional Description	26
4.0	Contractor Evaluation	47
4.1	Circuit Design Refinements	47
4.2	On-Aircraft Baseline & Implanted Defect Testing	48
4.3	SPADE Limit Calculations	72
4.4	SPADE Accuracy	75
5.0	Low Cost Sensor Development	95
5.1	On-Aircraft Testing	95
5.2	Laboratory Testing	95
6.0	Conclusions and Recommendations	106
6.1	Conclusions	106
6.2	Recommendations	108
References:		110

1.0 ABSTRACT

This report documents the design, development, and Prototype Field Evaluation of the Small Portable Analyzer Diagnostic Equipment (SPADE). The battery-powered SPADE is intended for flight line use in determining the condition of helicopter drive train bearings. It is designed and packaged to survive the army field maintenance environment and can be operated by semi-skilled personnel.

2.0 EXECUTIVE SUMMARY

2.1 Background - The SPADE (Small Portable Analyzer Diagnostic Equipment) program began in 1976 as a follow-on effort to some earlier testing of the "Shock Pulse" diagnostic technique. This earlier testing was conducted during the AIDAPS (Automatic Inspection Diagnostic and Prognostic System) program to evaluate a technique that is potentially more cost effective than vibration analysis for monitoring helicopter drive train bearings. The early testing of a commercial shock pulse instrument on UH-1 aircraft, plus implant testing on CH-47 gearboxes in test cells, gave promising results. These results showed the potential for designing an automated instrument that would be both simpler to build and operate as well as more accurate than a vibration pattern recognition system such as the AIDAPS prototype.

2.2 Technical Approach - The Shock Pulse Technique employed by the SPADE is a means of measuring the kinetic impact (shock) and frictional energy within a machine, independent of background vibration. This provides a highly accurate and trendable measurement of bearing condition that is independent of non-defect related background vibrations caused by the elastic motions of structures, rotors, gears, and shafts. The SPADE (see Figure 1) employs specialized signal conditioning and data processing techniques to measure frictional and shock energy associated with abrasive wear and dynamic impact of contaminated, pitted, spalled, corroded, or brinnelled bearing contact surfaces. This measured energy is then compared to preset limits (stored in the SPADE memory) that are representative of good, marginal, and discrepant conditions, and the status of the monitored

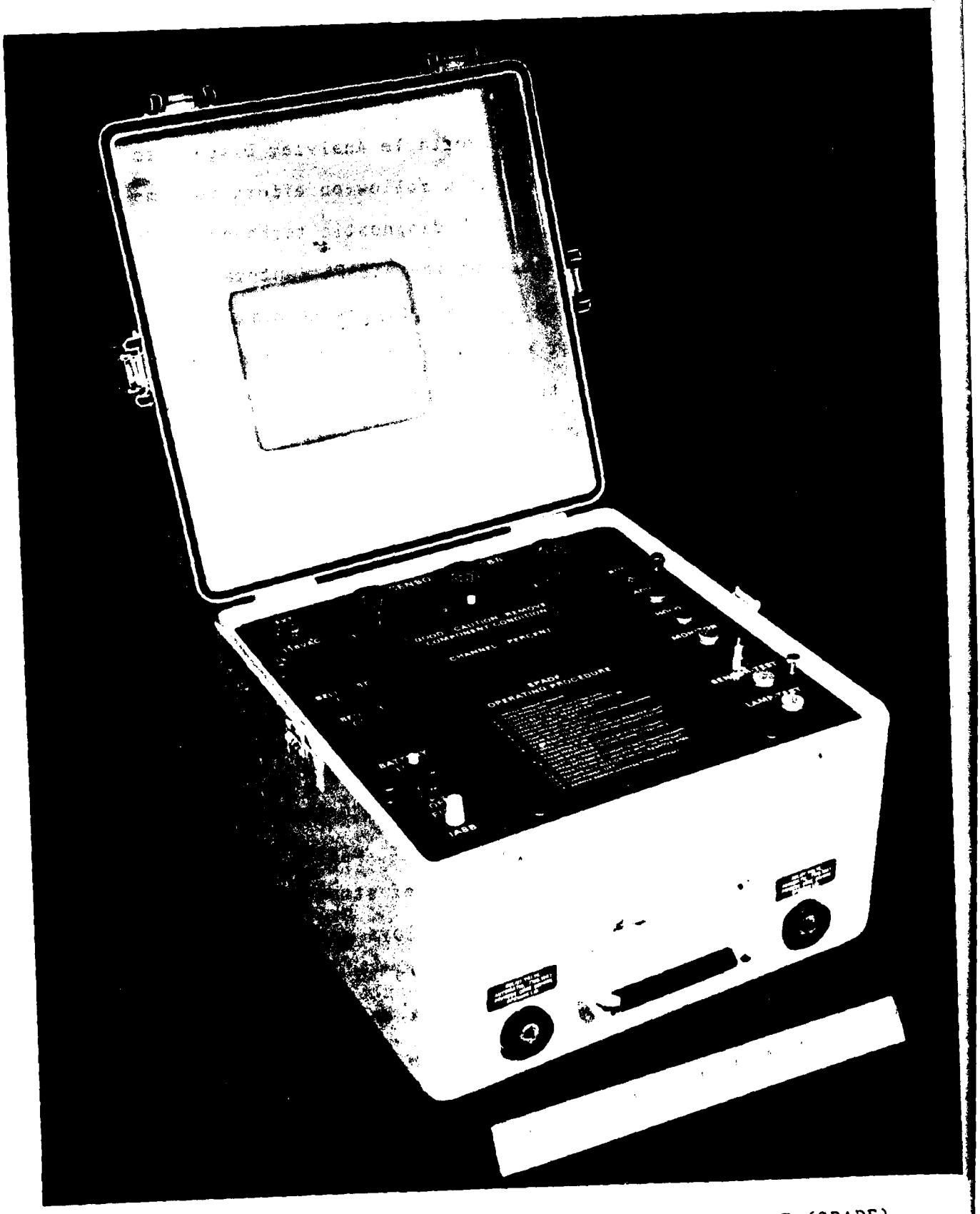

FIGURE 1 - SMALL PORTABLE ANALYZER DIAGNOSTIC EQUIPMENT (SPADE)

component is displayed on the instrument's control panel. The unit has sufficient internal memory capacity to automatically process data from up to twenty-two (22) sensor locations on each of eight different aircraft models. It provides component condition readout in the form of a green (good), yellow (caution), or red (remove) light and a two digit percent degradation display to allow trending of discrepent components in the yellow (caution) zone. It is designed and packaged to survive the army field maintenance environment and can be operated by semi-skilled personnel.

2. 3 Program Synopsis - The SPADE program was carried out in three chronological phases between September of 1976 and January, 1979 (see Table 1).

2.3.1 In Phase 1, a Sensor Location Study recommended where shock pulse sensors should be mounted on four (4) aircraft types (UH-1, AH-1, CH-47, and OH-58); the SPADE electronics were designed and breadboarded; a Bearing Test Fixture (BTF) was designed and fabricated; a SPADE Engineering Prototype was designed, fabricated, and laboratory tested using the BTF; and a successful Critical Design Review (CDR) was held in September, 1977.

2. 3.2 Upon completion of CDR, Phase II of the program was initiated to design, fabricate, and lab test three-field test prototypes that would be representative of production units in physical appearance and operation. This was completed in February of 1978, and Phase III began with the Contractor Evaluation of these three SPADE prototype units.

TABLE I

SPADE Program Synopsis

Phase	Task	Activity
I	1.	Sensor Location Study
	2.	a.) Circuit Design & Breadboard b.) Bearing Test Fixture Design & Fab. c.) Engineering Prototype Design, Fab. & Lab Test
CRITICAL DESIGN REVIEW		
II	1.	Field Test Prototype Design, Fab. & Lab Test
III	1.	Contractor Evaluation -- Lab, Test cell, & on-aircraft tests -- Circuit design refinements -- Sensor development
	2.	Field Test Support --Operation & AVUM Maintenance Manual --Training --Field Technical Support

2.3.3 The Contractor Evaluation included sensor and circuit design refinements and testing on the BTF in the laboratory, on a UH-1 42° gearbox in a test cell, on a UH-1 aircraft at Scott AFB, and on both UH-1 and AH-1 aircraft at Ft. Rucker. The Contractor Evaluation was completed in September 1978 and followed by the preparation of an AVUM level Operation & Maintenance Manual as well as several days of training for TRADOC personnel. Finally, during the FDTE at Ft. Hood, additional technical support was provided to reset warning thresholds when a new more rugged sensor type with slightly higher sensitivity was included in the testing.

2.4 SPADE Diagnostic Accuracy - The accuracy of any diagnostic technique or equipment must be judged from two points of view: 1.) the probability of calling a bad part bad, and 2.) the probability of calling a good part bad (a false failure indication). Both of these accuracy/inaccuracy figures increase as the diagnostic inspection frequency goes up.

2.4.1 Data from both implanted defects and baseline testing of the SPADE during the Contractor Evaluation, when conservatively evaluated, indicate that for a 25 flight hour usage interval, the SPADE cumulative probability of fault detection is 94% and would give a false indication only once per thousand flight hours on a UH-1 size aircraft. It should be pointed out that these accuracy levels exceed the objectives for OT-1 and essentially meet the objectives for OT-II.

2.4.2 These results also appear to be substantiated by the results of the FDTE conducted at Ft. Hood, Texas. During this testing, six (6) components were removed due to SPADE indications and subsequently disassembled to verify their condition. Only two components (an AH-1

rotor driveshaft hanger bearing and an AH-1 90° gearbox bearing) were found to be insufficiently degraded to justify removal. However, these removals were based on limits for the UH-1 aircraft which has a different tail boom/tail rotor configuration than the AH-1 . In addition, subsequent investigation showed visible scratches (that could be felt with a knife blade) from hard particle contamination of the 90° gearbox input quill bearings and that the hanger bearing indication was incorrectly obtained due to use of the M2 type of sensor with M3 type limits in the instrument's memory. Of the remaining four (4) correctly diagnosed bearing defects, three (3) were tail rotor driveshaft hanger bearings and one (1) was a 90° tail rotor gearbox bearing. None of these four (4) defects was detected by normal maintenance and inspection procedures.

2.5 Conclusions & Recommendations

2.5.1 Conclusions

1.) SPADE is an accurate, rugged, and simple to operate instrument for the diagnosis of bearing defects in helicopter drive trains (see Table II, Contractor Summary Review of the SPADE FDTE Final Report).

2.) Artificial implantation of defective bearings in "alien" drive train components may not produce levels of shock and frictional energy representative of these same defects in their "native" environment. This is most probably due to changes in the location and orientation of a surface damage area relative to the actual load zone of the bearing and the removal of trapped debris.

TABLE II

CONTRACTOR SUMMARY REVIEW OF THE SPADE FDTE FINAL REPORT (TRADOC TRMS NO. 9-F0194)

SPADE Critical Issue & Associated Criteria	FDTE FINDINGS Remarks and/or recommendations	Source	Contractor's Comments
Does SPADE have the capability for automatic diagnosis of bearing condition, thus minimizing unwarranted change of aircraft components?	Yes	USATSCH	
What is the diagnostic accuracy characteristic for SPADE when operated by military operators? SPADE indication of degraded bearings must be verified by teardown analysis to a minimum accuracy of 90%.	Seven components were removed from the aircraft at the test site, and sent to Corpus Christi, TX, for teardown analysis. One component (42° gearbox) cannot be located at CCAD.	USATSCH	Of the six components removed due to SPADE indications and subsequently disassembled to verify their condition, only two components (an AH-1 tail rotor drive shaft hanger bearing and a AH-1 90° gearbox bearing) were found to be insufficiently degraded to justify removal. However, both of these removals were based on limits for the UH-1 aircraft which has a different tail boom/tail rotor configuration than the AH-1. In addition, subsequent investigation showed visible scratches (that could be felt with a knife blade) from hard particle contamination of the 90° gearbox input quill bearings and that the hanger bearing indication was incorrectly obtained due to use of the M2 type of sensor with M3 type limits in the instrument's memory. Of the remaining four correctly diagnosed bearing discrepancies, three were tailrotor driveshaft hanger bearings and one was a 90° tailrotor gearbox bearings. All four cases showed varying degrees of bearing damage ranging from heavy spalling to surface scratches caused by hard particle contamination. None of these four defects were detected by normal maintenance and inspection procedures. Data from both implanted defects and baseline testing of the SPADE during the Contractor Evaluation indicate that for a 25 flight hour usage interval, the SPADE cumulative probability of fault detection is 94% and would give a false indication only once per thousand flight hours on a UH-1 size aircraft. It should be pointed out that these accuracy levels exceed the objectives for OT-1 and essentially meet the objectives for OT-II.
Does SPADE have a functional self-test capability?	Yes	USATSCH	
The prevailing environmental and weather conditions at the test site must not effect the system	Met. SPADE was operated from -4° centigrade (C) to +18° C and was operated in rain with no effect on the SPADE system	USATSCH	
Is SPADE sufficiently rugged, when packaged, to withstand ground vehicle transport over secondary roads and trails with minimal adverse effects?	Yes, SPADE was transported approximately 1000 miles in and around the test site with no adverse effects	USATSCH	

TABLE II (Cont'd)

Contractor Summary Review of the SPADE FDTE Final Report (TRADOC TRMS No. 9-F0194)

SPADE Critical Issue & Associated Criteria	FDTE Findings Remarks and/or Recommendations	Source	Contractor's Comments
Are SPADE and attachments portable, lightweight and easily carried by one person?	Partially met. It is portable but is too heavy and bulky	USATSCH	Significant reduction of SPADE weight and bulk can be achieved through design of a customized case. Such a custom design was not compatible with cost and schedule constraints of the SPADE prototype program.
Is SPADE capable of accomodating at least 20 test points without relocating the equipment?	Unknown. Only ten points were used during FDTE. This did not require the SPADE to be repositioned.	USATSCH	SPADE is fully capable of monitoring up to twenty-two (22) sensor locations on any single aircraft. The only reason this has not been demonstrated is because there were only ten (10) useful sensor locations defined on the UH-1.
Can the sensors be attached to existing hardware by a simple, low cost method?	Yes	USATSCH	
Are wires and cables for sensor installation adequately supported to prevent hazardous operation and injury to personnel?	Yes	USATSCH	
Will SPADE operate for eight hours on battery power without recharging	Not met. The mean-time-between-battery charges is four hours, fifty-eight minutes. Suggest changing the Independent Evaluation Plan to read: "SPADE must operate for 4.5 hours without recharging the battery."	USATSCH	This criterio is not in the Letter Requirement (LR). The system was not designed to meet it.
Will the SPADE battery recharge from 110-115 volts alternating current (AC) 60 Hertz (Hz), and what is the length of time required for recharging the battery?	Yes, 16 hours.	USATSCH	
Is training literature suitable for user operation and maintenance tasks?	No, see results in Subtest 2.9 and Subtest 2.10	USATSCH	The Contractor concurs: Training literature and SPADE operation & maintenance manuals were hurridly prepared on a limited budget due to late notification of their necessity for this phase of the government testing.

TABLE II (Cont'd)

Contractor Summary Review of the PADE FDTE Final Report (TRADOC TRMS No. 9-F0194)

SPADE Critical Issue & Associated Criteria	FTDE Findings Remarks and/or Recommendations	Source	Contractor's Comments
Does SPADE resist rust, fungus corrosion and condensation?	Yes	USATSCH	
What is the reliability of the SPADE stated as a point estimate?	Mean-time-between-failure (MTBF) was 6.5 hours	USATSCH	Four of the six "failures" charged to SPADE were for having to recharge the battery. This involves no hardware malfunction or failure and should be considered as preventive rather than corrective maintenance. One of the two remaining failures was BNC connector pins being pulled out. This has been corrected in commercial hardware by using heavier duty cable and vendor assembly of the sensor wire harness. The last remaining failure was due to a piece of dirt trapped in the sealed electronics compartment of SPADE
What is the operational availability of the SPADE	Operational availability A_o= .761	USAAVNBD	
Will SPADE require significant modification to the basic aircraft structure for installation of sensors? Extensive modification must not be required.	Partially Met. Cowling modification	USATSCH	The modifications required to the tail rotor driveshaft and 90° gearbox couplings are small and do not involve modification of any basic aircraft structure. In addition, it may be feasible to relocate or redesign the sensor mounting pads so that no cowling modification is required.
Is SPADE capable of testing of the UH-1H/AH-1 helicopter monitored components within 30 minutes after installation of the system?	Met. The time required to test an aircraft with all channels reading green is four to six minutes. The total time required to remove cowlings plus install and torque sensors on a UH1 aircraft is 19 to 24 minutes.	USATSCH	

3.) Some of the Shock Pulse Sensors used in this program did not meet the intent of the specification developed for their procurement. This resulted in some sensor sensitivity variations that were incompatible with full interchangeability of sensors. A revised procurement specification and acceptance test procedure has been developed to prevent reoccurance of this problem (See section V of this report).

4.) The testing and evaluation conducted to date has not provided a sufficient data base to make quantitive estimates of SPADE's prognostic capability (how SPADE readings change as a function of the level of damage or "remaining safe life" of a discrepant bearing). This type of information is key to determining the optimum utilization interval and operational philosophy for cost effective employment of SPADE in the army aviation environment.

2.5.2 Recommendations

1.) A SPADE Production Prototype program should be initiated to:

a.) Redesign packaging for improved portability;

b.) Finalize printed circuit board layout and design.

c.) Add capability for SPADE to operate from 28VDC aircraft power;

d.) Fabricate four (4) Production Prototype SPADE units for use in acquiring additonal baseline data, an R & M data base, and definition of prognostic as well as additional (non-bearing) diagnostic applications

2.) The baseline data collection program should be continued to refine sensor locations and further define SPADE alarm thresholds for the following aircraft drive systems: UH-60, CH-47 D, YAH-64, AH-1, UH-1, OH-58, and OH-6. This data collection effort should include teardown inspection of components identified as suspect from analysis of SPADE data and documentation of SPADE Production Prototype reliability and maintainability characteristics.

3.) An expanded testing program should be initiated to define SPADE prognostic capabilities as well as non-bearing diagnostic applications. Selected discrepant specimens found during baseline data base expansion should be run to failure in a test stand environment (without prior disassembly to verify the original diagnosis). SPADE readings accumulated during this destructive testing should be trended to establish SPADE's advance warning time and the rate of failure progression in bearings. Definition of expanded diagnostic applications for SPADE should concentrate first on detection of gear damage, second on diagnosis of defects in the rotating components of turboshaft engines, and third on monitoring hydraulic system components for internal leakage, cavitation, and pump bearing damage.

3.0 SPADE Design, Development, & Lab Test - This section will begin with a discussion of the basic technical principles of "Shock Pulse" analysis, upon which the operation of SPADE is based. It will continue with a narrative account of the hardware design, development, and lab test process; and conclude with a functional description of the SPADE Field Test Prototype.

3.1 Shock Pulse Analysis - Over the past decade there has been a continuing demand for higher levels of equipment availability and less unscheduled downtime. This has led to R & D for improved methods of fault detection and failure prediction. As a part of this diagnostics research effort, vibration analysis has been receiving renewed emphasis as a means of monitoring rotating machinery for discrepant operating and mechanical conditions. It has been through this recent research that two principle methods of vibration analysis have evolved. These two methods are frequently referred to as low frequency vibration analysis (or pattern recognition) and high frequency vibration analysis (or shock pulse monitoring). Extensive military and industrial experience with shock pulse monitoring has demonstrated high signal to noise ratios and timely warnings for failure modes as diverse as planetary bearing spalls and through-the-part cracks in gears and shafts. This section will discuss shock pulse theory,and illustrate its use through case histories.

3.1.1 Background - The terms "high" and "low" frequency refer to that portion of the overall vibration spectrum in which energy is monitored. Low frequency vibration analysis for rotating machinery will always include that portion of the transducer signal which contains the dynamic event frequencies of the machinery (the 0 to 10 KHz band). Some sort of processing may be performed on the low frequency signal;

for example, spectrum analysis; but the processing technique will deal specifically with the amplitudes of the dynamic event frequencies and their lower harmonic orders. High-frequency vibration analysis, on the other hand, utilizes the transducer resonant output at frequencies several orders of magnitude above the dynamic event frequencies of the machinery. It is this difference in "operating frequency" that makes the shock pulse technique insensitive to background vibration, but highly sensitive to the kinetic and frictional energy generated by defects in rotating machinery. Before proceeding with a detailed description of high frequency shock pulse techniques, it will be helpful to review the major elements of low frequency vibration analysis.

3.1.2 Low-frequency-vibration analysis is performed by spectrum analyzing the output of an accelerometer over a frequency range that includes the fundamental and lower harmonic dynamic event frequencies characteristic of a machine in normal operation. (These frequencies include rolling element pass frequencies over points on bearing races, gear mesh frequencies, and rotational frequencies of gear-shafts, bearing cages, planetary gear carriers, etc.) Thus for low frequency vibration analysis, accelerometer data above 10 KHz in the frequency spectrum is ignored. Diagnosis is based upon pattern changes; a baseline spectrum is recorded for each good machine and subsequent spectra are then compared to the baseline for significant deviations that can be considered indicative of component deterioration.

The problems that arise with this technique are:

How to implement simple field recording and storage of custom baseline data in such a manner that frequent rebaselining does not occur after fault detection

(similar to cleaning and reinstalling a chip detector).

Calibration and maintenance/replacement of flat-response accelerometers in a field/operational environment.

The tendency for low-frequency vibration patterns to change significantly due to normal variations of operational parameters (temperature, load, bolt torques, oil quality and viscosity, etc.).

Due to the nature of some machine vibrations, the dynamic event frequencies often appear as modulations of some powerful structural/rotational system resonance rather than discrete defect frequencies, the latter often being obscured by other stronger components in the signal.

3.1.3 Shock pulse analysis operates on the principle that discrepant parts within a machine (such as pitted, spalled, brinnelled, or skidding bearing elements) release abnormal amounts of frictional and/or kinetic energy. In the frequency domain, friction generates "white" noise (nearly constant amplitude at all frequencies up to several hundred KHz) and a kinetic event, by virtue of its very short rise time, generates only very gradually decaying amplitudes as a function of increasing frequency. The harmonic amplitudes of machine vibration, however, decay more rapidly with increasing frequency. Thus, above a certain frequecy, f_E, the amplitude of

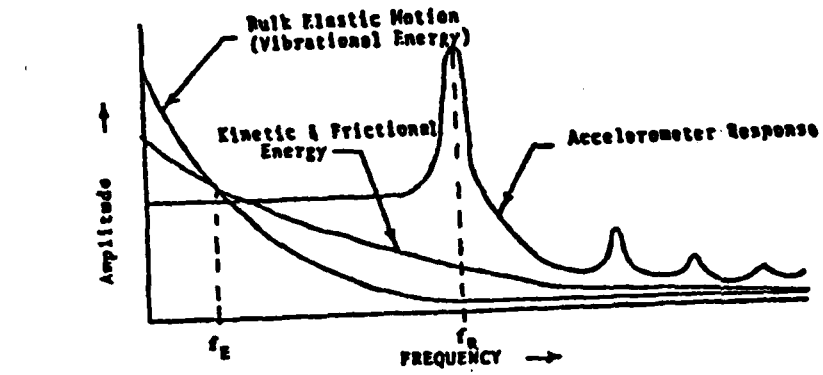

f_E - The frequency at which the energy from bulk elastic motion is equivalent to the energy from kinetic events and friction.

f_R - The accelerometer resonant frequency and the band-pass filter center frequency.

Δf_R - Band-pass filter width.

T_D - Time period between defect caused dynamic events.

f_D - Modulation frequency due to defect.

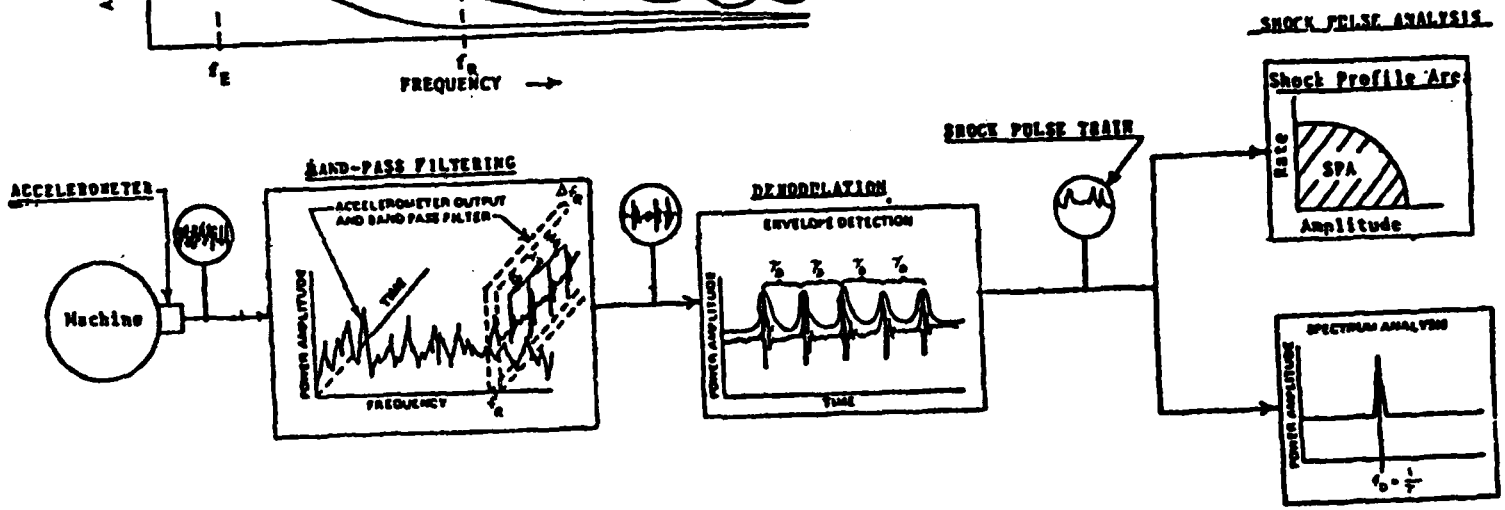

1) Kinetic and frictional energy is released by discrepant parts.

2) Kinetic and frictional energy decays less rapidly than vibrational energy in the frequency domain. Thus at frequencies greater than f_E, there is more kinetic and frictional energy than vibrational energy.

3) The accelerometer's resonant response amplifies kinetic and frictional energy at frequency f_R, which is greater than f_E.

4) The bandpass filter eliminates non-resonant response of the accelerometer, and the envelope detector follows the amplitude modulations of the accelerometer resonance (shock pulses).

5) The SPADE* Central Processor Unit (CPU) calculates the Shock Profile Area (SPA) and compares it to predetermined limits.

6) A spectrum analyzer displays the relative amplitude of shock pulses as a function of the frequency at which they occur.

* Small Portable Analyzer Diagnostic Equipment (SPADE) is an automated shock pulse instrument developed for flight line use on army helicopter drive trains.

Figure 2 - Shock Pulse Analysis Techniques

frictional and kinetic energy release will be greater than that of machine vibration. (This is depicted in Figure 2)

Additionally, a piezoelectric accelerometer has a resonant frequency that is typically greater than f_E, so that it can selectively amplify the high frequency kinetic and frictional energy it detects when mounted on a machine's housing. A bandpass filter on the accelerometer output, screens out transducer response at all frequencies significantly above or below the sensor's resonant frequency. This means that the time domain amplitude modulations of the bandpass filter output are almost entirely a function of kinetic and frictional energy fluctuations in the machine. An envelope detector follows the amplitude modulations of the bandpass filter output, thus providing a "Shock Pulse" each time the accelerometer is resonated by the release of kinetic and frictional energy.

This shock pulse signal can be analyzed in several ways - the two most effective of which are Shock Pulse Spectral Analysis and Shock Profile Area Measurement. In Shock Pulse Spectral Analysis the shock pulse train is fed into a conventional narrow band spectrum analyzer which performs a Fourier transformation and displays the relative amplitude of shock pulses as a function of the frequency at which they occur. In Shock Profile Area Measurement, the shock pulses are analyzed to construct a curve of shock pulse rate as a function of the shock pulse absolute amplitude. This curve is called a "Shock Profile", and the area under the curve, which is proportional to the total kinetic/frictional energy release within the machine, is called the "Shock Profile Area" (SPA). Thus the SPA

is a diagnostic parameter capable of detecting discrepant parts whose failure modes generate abnormal levels of kinetic and frictional energy. Each of these two analysis methods has advantages and disadvantages summarized briefly as follows:

Shock Profile Area Measurement

Advantages: Sensitive to both periodic and non-periodic kinetic and frictional energy release, provides the simplest means of monitoring level of degradation, can be implemented with a simpler and lower cost electronics than required for spectrum analysis.

Disadvantages: Cannot provide detailed fault isolation within a component nor discrimination between failure modes (i.e. lube contamination vs. localized surface damage in a bearing, or tooth spalling vs. through-the-part crack in a gear).

Shock Pulse Spectral Analysis

Advantages: Provides through-the part gear crack detection (See Figures 3 and 4), detailed fault isolation capability within a monitored component or assembly (i.e. spalled outer race of bearing XXXXXXX in output quill of No. 1 turbine transmission) and provides earliest indication of very small amounts of debris or localized surface damage.

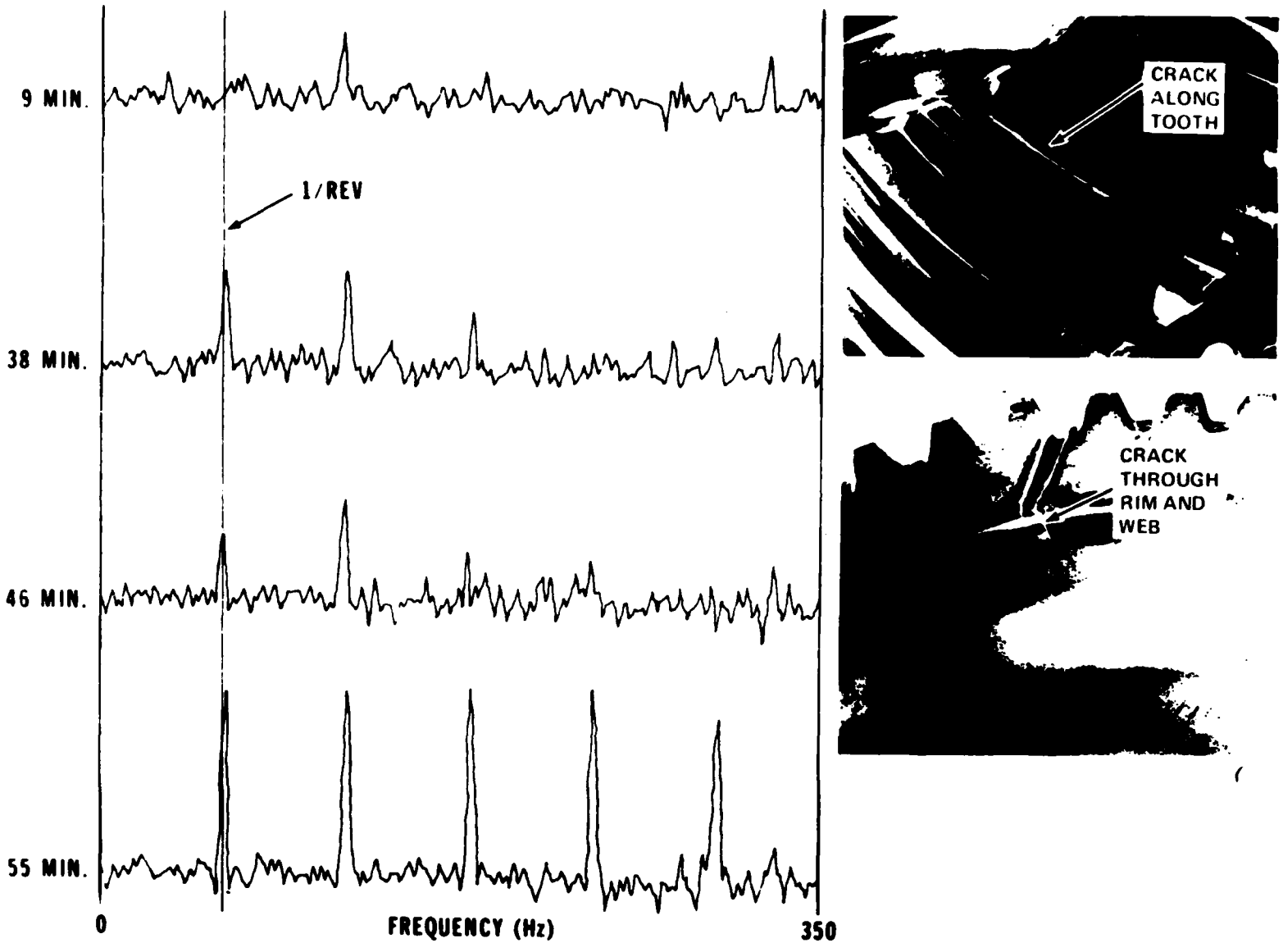

FIGURE 3 - SHOCK PULSE ANALYSIS OF CRACKED SPIRAL BEVEL GEAR (IN TEST STAND)

(NOTE: This data taken from Reference 1)

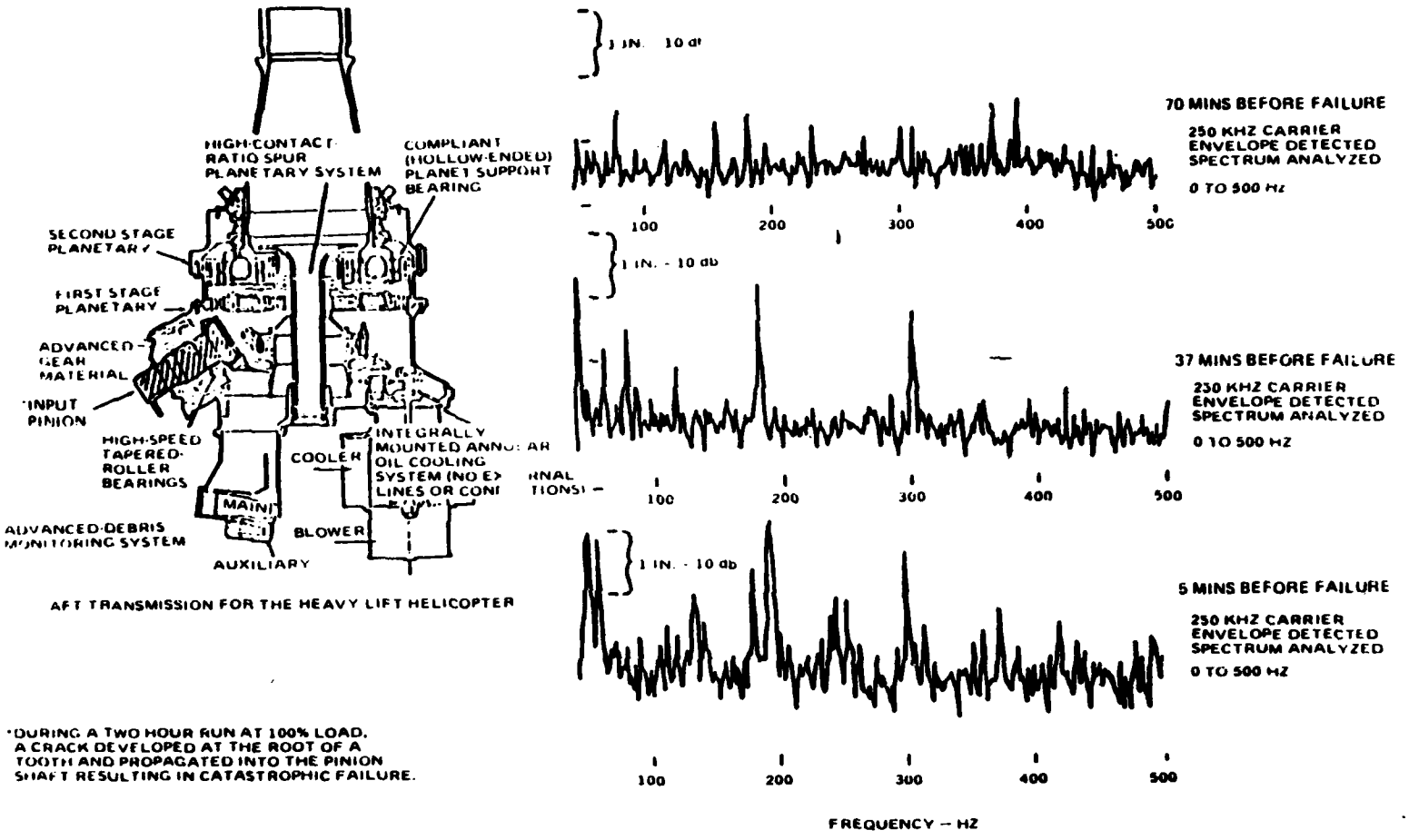

AFT TRANSMISSION FOR THE HEAVY LIFT HELICOPTER

*DURING A TWO HOUR RUN AT 100% LOAD, A CRACK DEVELOPED AT THE ROOT OF A TOOTH AND PROPAGATED INTO THE PINION SHAFT RESULTING IN CATASTROPHIC FAILURE.

FIGURE 4 - HEAVY LIFT HELICOPTER SPIRAL BEVEL GEAR CRACK DETECTION

(NOTE: This data taken from Refernece 2)

Disadvantages: Insensitive to very large (50% of race area) continuous bearing spalls (see Figure 5, case No. 7) and to all non-periodic dynamic/frictional energy sources such as unfiromly distributed bearing wear, heavily contaminated lubricant, and continuous rubbing contact due to loose or deformed retention and mounting hardware.

Obviously, these two methods of analyzing the shock pulse signal are highly complementary so that when used together they offer dramatic diagnostic capabilities in terms of fault detection, fault isolation, and failure progression monitoring. Other methods of analyzing the shock pulse signal are also useful; such as RMS and crest factor (peak to RMS ratio) measurement. However, while these additional methods have advantages in terms of hardware cost, they have certain disadvantages in signal to noise ratio and fault isolation capability. Regardless of which of these shock pulse analysis methods is employed, the high frequency shock pulse technique has the following important advantages over traditional low frequency analysis:

Custom baselines are not required. A "Generic Baseline" (a common baseline for all units of the same part number) can be employed for fault detection even in components as dynamically complex as a helicopter rotor transmission. (See Figure 5).

AFT TRANSMISSION

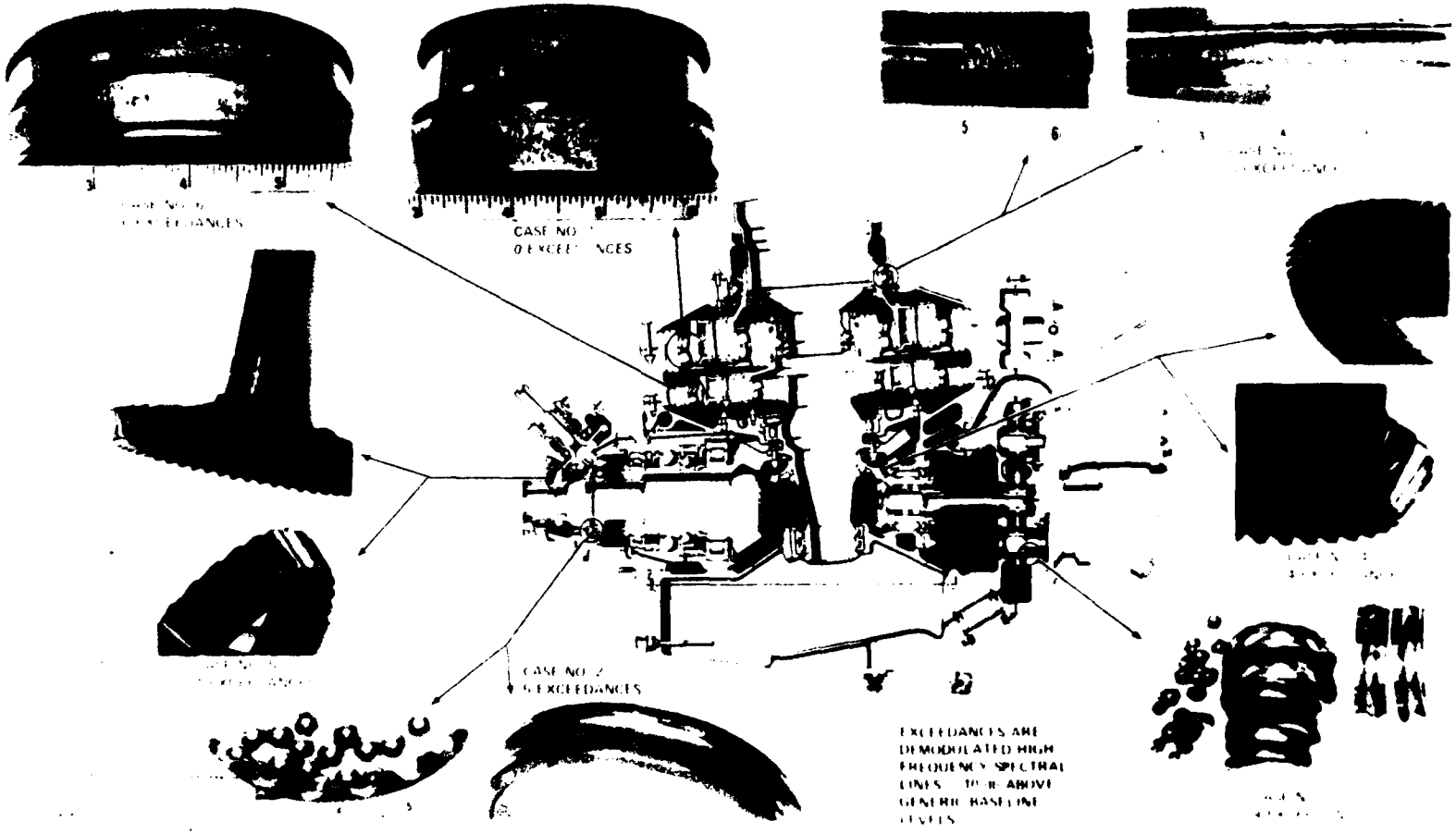

FIGURE 5 - SHOCK PULSE SPECTRAL ANALYSIS OF CH-47 HELICOPTER ROTOR TRANSMISSION
(NOTE: This data taken from Reference 3)

High signal to noise ratio demodulated high frequency vibration patterns are relatively insensitive to normal variations of operational parameters, but show dramatic sensitivity (10 db signal growth) to relatively small levels of degradation. (See Figure 6).

The SPADE employs the Shock Profile Area (SPA) method for the following reasons:

1.) Fault detection (including failure modes that do not cause periodic (shock pulses) and failure prediction are more important in the Army Aviation maintenance environment than minor defect detection and detailed fault isolation capability.

2.) The cost of analog signal conditioning and digital data processing circuitry is significantly less when spectral analysis is not required.

3.2 SPADE Hardware Design & Development - The SPADE hardware was developed in three steps, breadboard, engineering prototype, and Field-Test Prototypes. During the first step, the design of the SPADE Electronic Unit (EU) circuitry progressed on paper while it was checked by "breadboarding" as shown in Figure 7. When the major signal conditioning and data processing circuitry had been designed and the breadboard circuits successfully tested on the Bearing Test Fixture, step two was initiated to construct an Engineering Prototype unit.

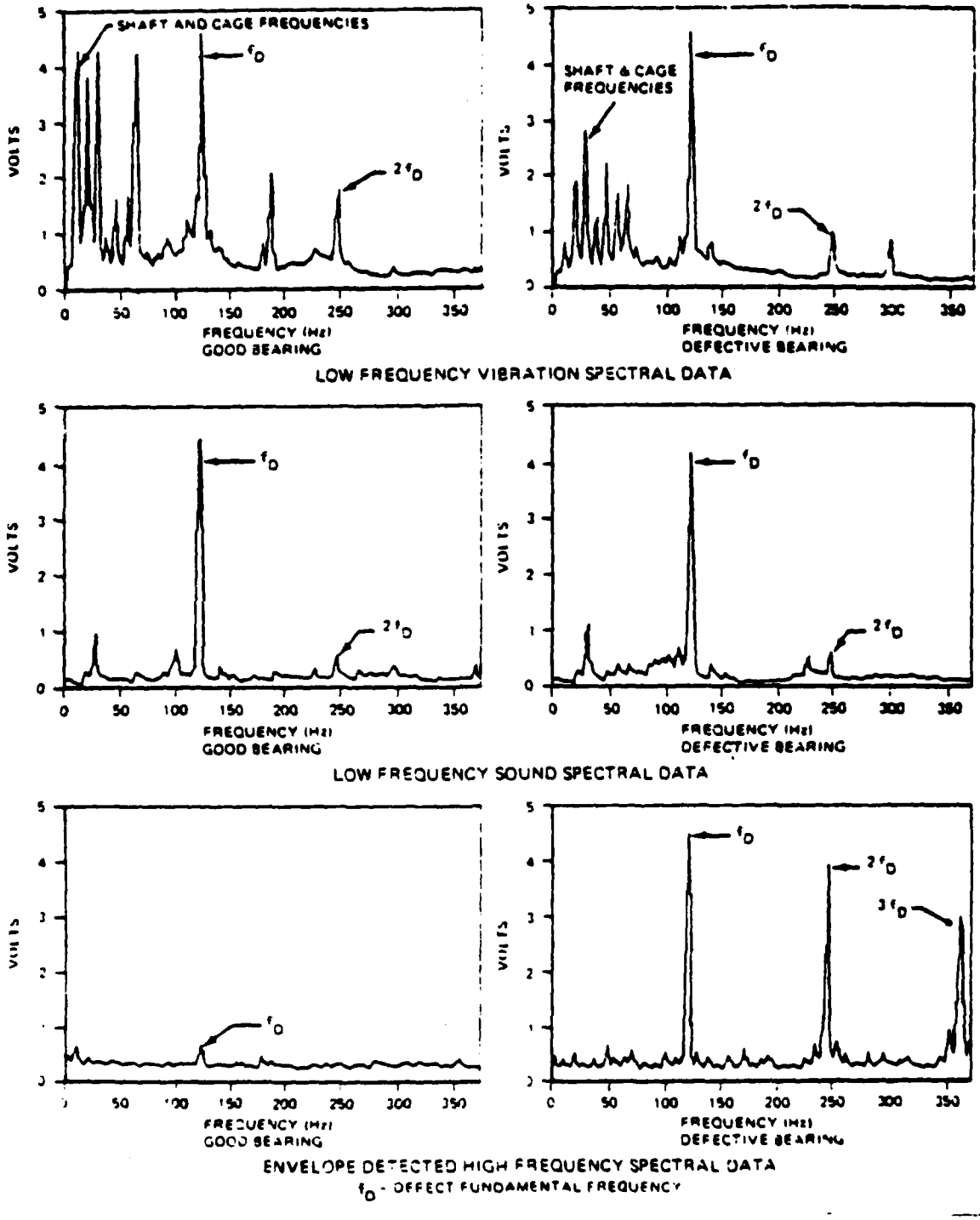

FIGURE 6 - COMPARISON OF VIBRATION, SOUND, AND SHOCK PULSE DATA

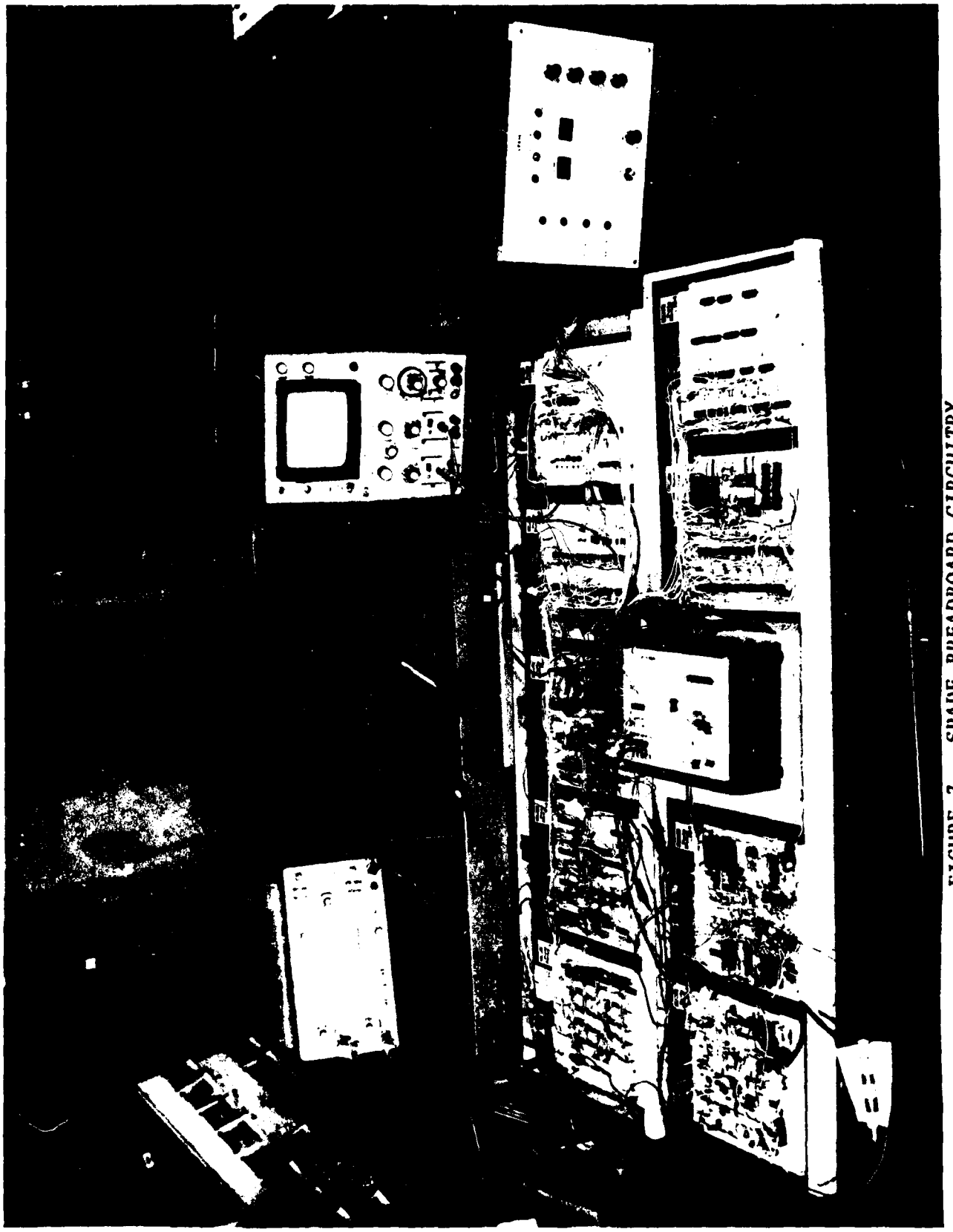

FIGURE 7 - SPADE BREADBOARD CIRCUITRY

In this unit the "breadboarded" circuit design developed during step 1 was fabricated on Printed Circuit Boards (PCB's) that were representative of their configuration in the Field Test Prototypes to be constructed during step 3. Power supplies, batteries, lights, switches and all other electronic hardware components were selected to assure maximum functional commonality between the Engineering Prototype and the Field-Test Prototypes to come. However, primarily due to program cost and schedule constraints, the Engineering Prototype's case and packaging were not representative of those planned for the Field-Test units (see Figure 8).

After successful demonstration of the Engineering Prototype during the Critical Design Review (CDR), it was decided to proceed with the fabrication of three (3) Field-Test Prototypes for contractor and government testing. Five months after this CDR approval to proceed, the first Field-Test Prototype began contractor evaluation at Ft. Rucker, Alabama. During the contractor evaluation, circuit design refinements (as described in section 4.1) were developed, incorporated, and evaluated prior to delivery of the three field test prototypes for government testing.

3.3 SPADE Field-Test Prototype Functional Description

3.3.1 Introduction

The SPADE Shock Pulse Analyzer is a piece of diagnostic test equipment that functions on the principle of detecting and measuring shock pulses generated by the release of kinetic and frictional energy within monitored components. The analyzer is insensitive to mechanical vibrations, and calculates Shock Profile Area (SPA), which

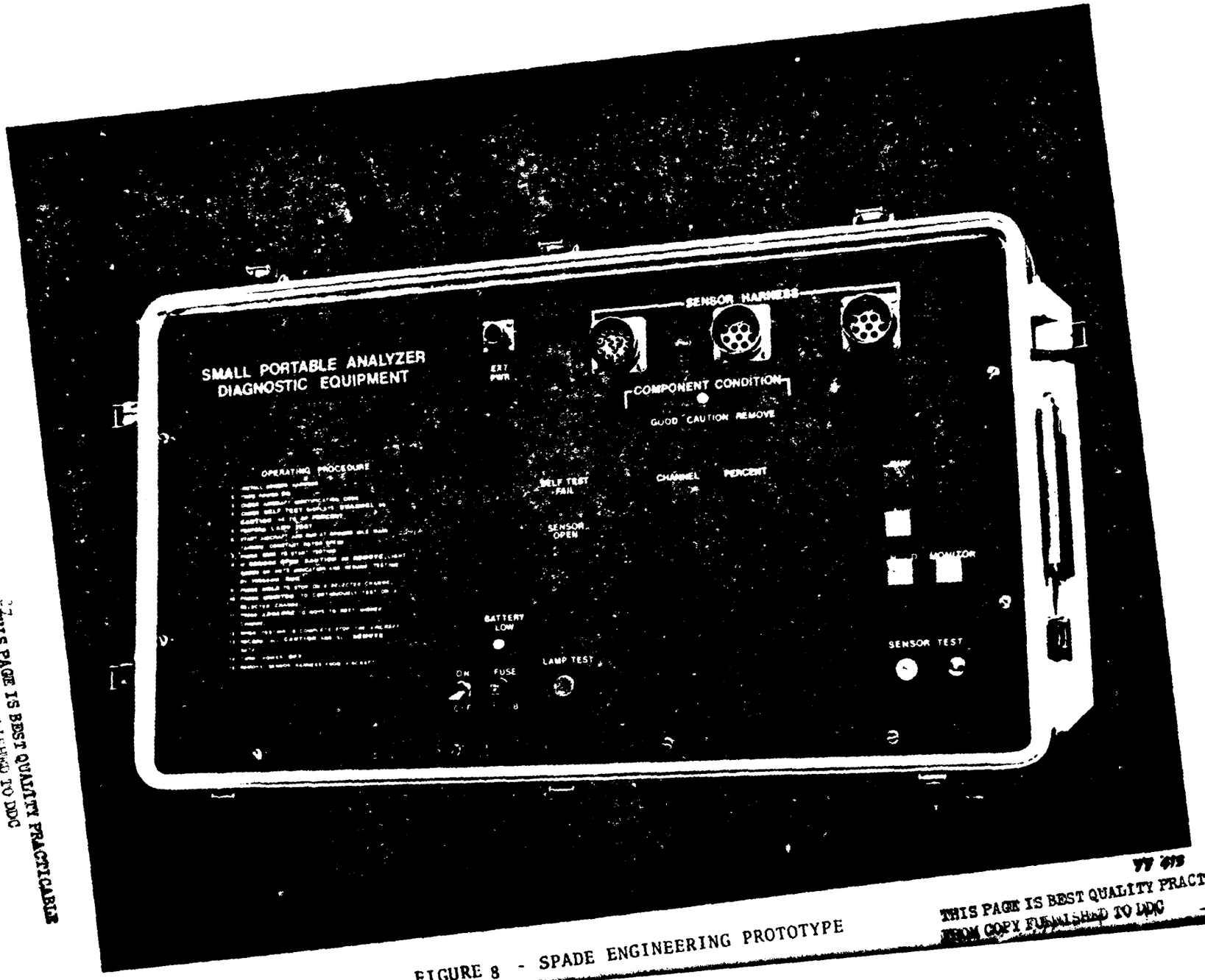

FIGURE 8 - SPADE ENGINEERING PROTOTYPE

THIS PAGE IS BEST QUALITY PRACTICABLE
FROM COPY FURNISHED TO DDC

is proportional to the total kinetic and frictional energy release within a component. The measured SPA is then compared to preset limits (stored in the Shock Pulse Analyzer memory) that are representative of good, marginal, and discrepant conditions, and the status of the monitored components is displayed on the instrument's control panel.

3.3.2 SPADE Operating Procedure

The SPADE is a piece of diagnostic test equipment to be used prior to scheduled periodic maintenance, or prior to unscheduled maintenance on rotating machinery as a means of defining bearing conditions in that machine. To use the instrument, a mechanic must first install each sensor and sensor cable according to the pre-assigned cable numbers on each connector. After the connectors are hooked up to the instrument, the operator turns on power, checks the self test displays (generated automatically by power initiation), and performs a LAMP TEST by pushing the appropriate button on the Shock Pulse Analyzer control panel.

To begin testing, the aircraft under investigation must be ground-run at flat pitch for a sufficient period of time (10 min.) to stabilize operating torques, speeds, and temperatures in the rotating components. To initiate processing of shock pulse data the operator must momentarily depress the RUN pushbutton.

The instrument will automatically sequence thru each sensor location until an abnormal energy level is detected. If an abnormal condition is detected, the automatic processing will stop, the channel number will be displayed, and the appropriate CAUTION (Yellow) or REMOVE (Red) component condition is indicated. The PERCENT display will also indicate the approximate level of degradation from a good bearing to a bearing requiring removal.

For continuous processing at one sensor location the operator must first press the HOLD pushbutton to stop processing and then press MONITOR. This will allow data to be updated every 15 seconds on the selected channel. (Note: If the instrument has already

stopped processing due to a CAUTION or REMOVE indication, the MONITOR may be entered directly without first pressing HOLD). To exit the MONITOR mode and continue processing on the remaining sensor channels the operator must first press HOLD (to stop the MONITOR function) and then press RUN. When data has been processed from all sensor locations, the operator can manually step through each channel using the ADVANCE pushbutton and note abnormal conditions as they are displayed from the instrument's memory.

The testing is now complete, power can be turned off, and the sensors/cables removed.

3.3.3 General Configuration

The SPADE Electronic Unit can be functionally divided into seven (7) major areas:

1. Control Panel
2. Input Multiplexer (MUX) and Scaler
3. Self Test Generator (STG)
4. Input Amplifier Pulse Generator (IAPG)
5. Central Processor Unit (CPU)
6. Sequencer
7. Display Memory and Drivers

Figure 9 illustrates the interrelationship of each of these seven (7) functional areas. The following discussion provides a more complete description of the detailed functions within the above seven (7) major areas.

3.3.4 Control Panel

The control panel provides contol inputs to the SPADE and displays the status and results of testing. The control switches

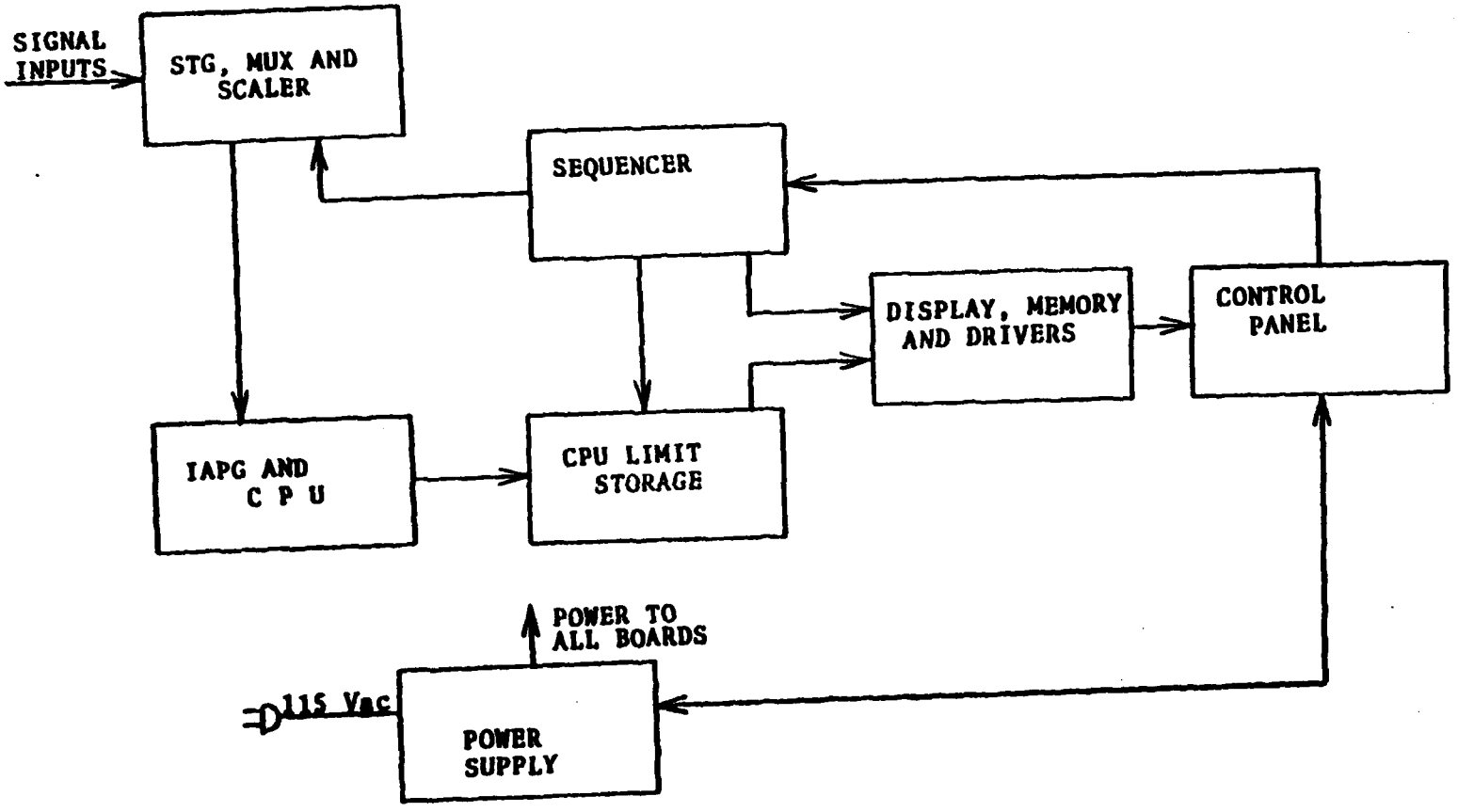

FIGURE 9 - SPADE ELECTRONIC UNIT (EU) FUNCTIONAL RELATIONSHIPS

operate the power supply and sequencer. The displays indicate the condition of the battery, channel identification, and test status from the display memory and drivers (see Figure 10).

The Power Switch enables power to the Shock Pulse Analyzer. The RUN pushbutton enables the sequencer to scan and process channels consecutively until a non-pass condition is met. Momentarily depressing the ADVANCE pushbutton allows the CHANNEL display to advance by one count and indicate the status of that channel's last reading. Holding the ADVANCE switch depressed allows a one-half second scan of each channel after an initial two second wait. NOTE THAT IN THE ADVANCE MODE ONLY "OLD" DATA IS DISPLAYED AND NO "NEW" DATA IS PROCESSED. Depressing the MONITOR pushbutton allows the selected channel to be real time monitored while "new" data is processed and the display status updated each CPU cycle. The HOLD pushbutton manually stops the RUN function or MONITOR function.

The CHANNEL display shows the two digit address of the last channel processed, and all status indicators pertaining to this channel. If the CPU is processing a new set of data, the CHANNEL digits (corresponding to the previous data) blink. The GOOD (green) indicator represents a healthy component, the CAUTION (amber) indicates a marginal condition, and the REMOVE (red) light indicates a discrepant part. If upon power initiation, the channel 0 reading is outside the range of 40% to 60% in the caution zone, the SELF TEST FAIL (red) indicator will light. This is to indicate a malfunction in Shock Pulse Analyzer circuitry. The SENSOR OPEN indicator shows that insufficient input signal amplitude is available for processing and indicates a malfunction in hookup, a bad accelerometer, cable or input channel.

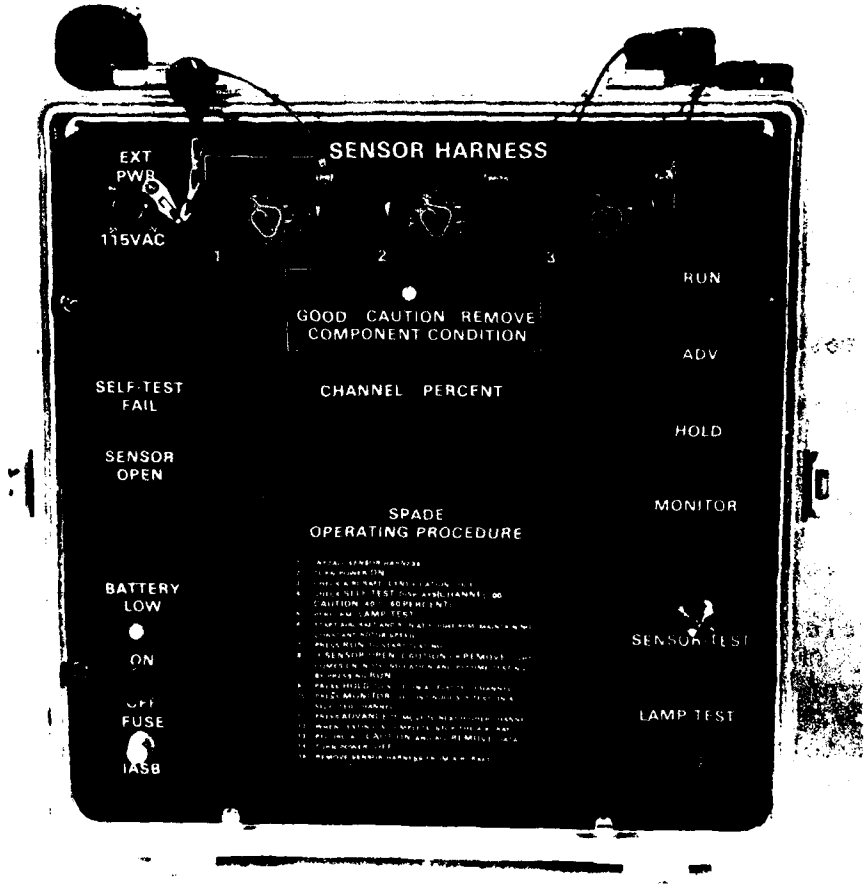

FIGURE 10 - SPADE CONTROL PANEL

A sensor test pushbutton and mounting stud are located on the Control Panel to test any questionable accelerometers. This is accomplished by attaching the accelerometer onto the stud and connecting it to the special connector designated for channel 23. The SENSOR TEST pushbutton, when depressed at channel 23, will cause a CAUTION indication of 20 to 50% if the accelerometer is functioning properly.

3.3.5 Input Mux and Scaler (MUX)

The Input Mux and Scaler interfaces with accelerometers and the self test generator (STG) for inputs and, under sequencer address, switches a selected input to the Input Amplifier Pulse Generator (IAPG). The accelerometer signals are supplied through coaxial cables of varying length to the MUX. The scaler gain normalizes these accelerometer signals and the MUX allows the selected signal to appear on the MUX data bus while shunting all other input signals to ground to minimize crosstalk. The output signal on the data bus is supplied to the IAPG.

Functional Description and Signal Flow

Referring to Figure 11 the input MUX and scaler is composed of 31 scaler circuits for the 30 data inputs, and one accelerometer test input; one self test input; and an address decoder for the 32 channel MUX.

Each scaler circuit consists of a cable terminating capacitor and a series signal limiting resistor. The capacitor is the scaling factor used to compensate for the variations in cable length. The cable used in the Shock Pulse Analyzer application

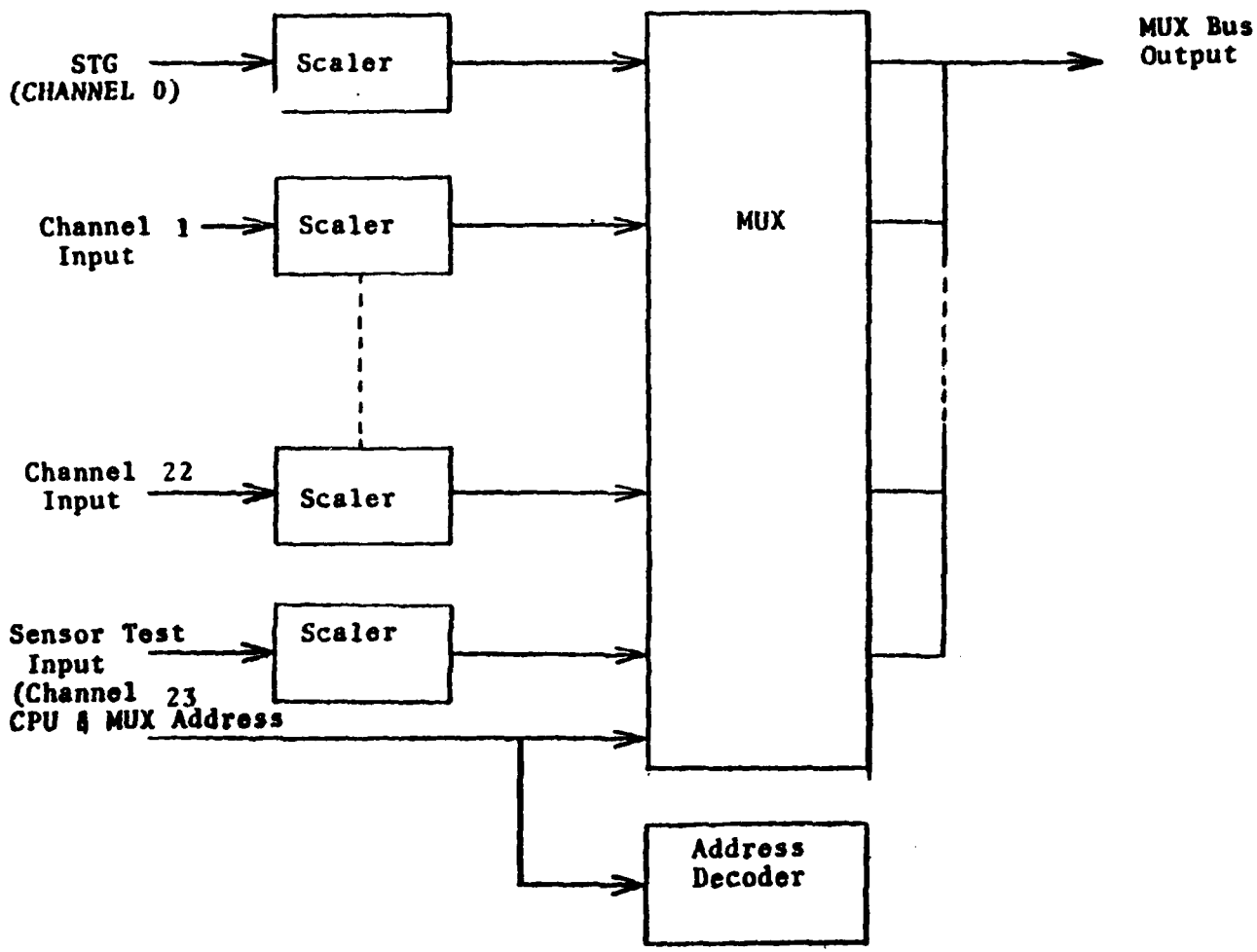

FIGURE 11 - INPUT MUX & SCALER FUNCTIONAL BLOCK DIAGRAM

(RG180B/U) has a capacitance of 14.5 pf per foot. For a variation of the shortest to longest cable length of 50 feet, the capacitance difference would be 725 pf. Since the accelerometer appears as a capacitive source in the range of 1000 pf the varying cable length capacitance would cause varying attentuation of the accelerometer's detected signal. Thus, a scaling capacitor is used on each channel input to gain normalize the signal passed on thru the MUX to the IAPG. The series resistor presents a shunt load of 10K across the accelerometer for a non-selected MUX channel (explained below) and acts as a circuit protecting current limiting device for the MUX CMOS switches during excessive signals and when power to the Shock Pulse Analyzer is off.

The address decoder when addressed disables the shunt switch of the selected channel while enabling all other shunts.

The MUX consists of 32 series shunt CMOS solid state switch combinations. Each channel utilizes one switch from a DG508A integrated circuit that passes the input signal from the scaler to the MUX bus when selected, and one switch from a DG201A integrated circuit that shunts the scaler signal to grount when not selected. The DG508A switch has a typical ON to OFF isolation of 80db or 10,000 to 1.

3.3.6 SPADE SelfTest Generator (STG)

The STG is connected directly to MUX channel 0 and provides a simulated accelerometer input signal to that channel. In addition, the STG generates a physical pulse that can be used as a mechanical input to verify accelerometer operation.

The STG is free running and the simulated signal is automatically energized only when the SPADE is operated in channel 0 (for instrument self test) or when the sensor test pushbutton is depressed. Channel 23 has been allocated with known limits for testing sensors.

Functional Description

Referring to Figure 12, the STG is composed of an asymetric bistable oscillator, a resonant tank circuit and a pulse generating crystal assembly. The bistable utilizes a standard 555 type timer to generate microsecond duration pulses at a fixed rate.

This pulse train is applied to an L-C tank circuit to produce a damped second order resonance simulating a pulsed accelerometer resonant output. This signal is amplified and provided with source impedance simulating that of an accelerometer to channel 0.

The bistable output pulse is resistively divided and used as a direct input to drive a crystal coupled to a mounting stud on the front panel. This arrangement provides a mechanical output pulse that can be coupled to any one of the measurement accelerometers used with the Shock Pulse Analyzer to determine if it is functioning. Channel 23 has been reserved to perform this test.

The STG operation is controlled by an inhibit applied to the bistable oscillator. In channel 0 the solid state switch controlling the inhibit to the pulse generator is de-energized. In other MUX channel address configurations the switch is energized, causing the oscillator to cease operation. An exception to this occurs when the SENSOR TEST pushbutton is depressed. This enables the pulse generator and activates the sensor stud on the control panel.

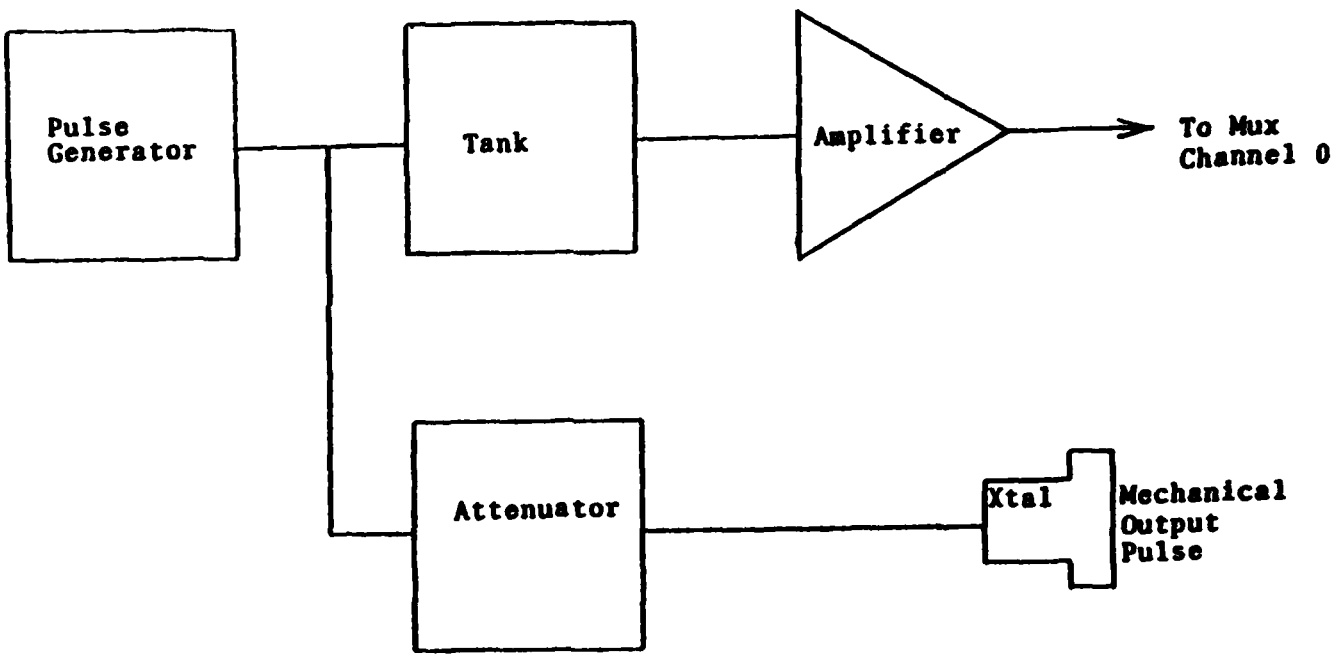

FIGURE 12 - SELF TEST GENERATOR (STG) FUNCTIONAL BLOCK DIAGRAM

3.3.7 Input Amplifier Pulse Generator(IAPG)

The IAPG interfaces with the MUX for inputs and outputs to the CPU. The MUX switches basically raw (but gain normalized) unconditioned signals from the accelerometer into the IAPG. The IAPG conditions the filtered portion of the signal that contains damped bursts of the accelerometer resonant frequency and determines the envelope of that signal. This filtered and demodulated signal is the Shock Pulse Train which is fed to the CPU.

Functional Description

The IAPG signal input from the MUX data bus is fed into a tuned tank circuit which resonates at approximately 40 KHZ. It is the property of a tank circuit to have its greatest impedance at its resonant frequency because the existance of circulating currents with the tank circuit minimizes the amount of signal sourced current that will be drawn into the tank. At other frequencies, the impedance presented by the tank is markedly lower than at resonance. The effect of impressing the tank circuit across the accelerometer as a load is to greatly reduce the gain of the accelerometer at any frequency other than at the tank circuit resonance thus acting as a band-pass filter.

By tuning the tank circuit to the resonanct frequency of the accelerometer, all low frequency vibration energy is eliminated while high frequency "bursts" of kinetic and frictional energy will be present in sufficient strength to be detected. This band-pass filtered signal is then half-wave rectified and low-pass filtered to provide a de-modulated accelerometer resonance (shock pulse) signal for input to the Central Processing Unit.

3.3.8 Central Processing Unit (CPU)

The CPU inputs signals from the IAPG and processes them to determine the Shock Profile Area (SPA). Data is accumulated for a period of 15 seconds and is fed to the CPU Limit Storage (CLS) board. Here the data is compared to preprogrammed limits and the results are sent to the display memory and driver board.

Functional Description

Figure 13 shows a block diagram of the CPU. Shock Pulses from the IAPG are fed to a digital processor where the Shock Profile Area (or total shock pulse energy content) is computed. This is accomplished by converting the shock pulse signal to digital form, calculating the energy content of individual pulses, and accumulating the total shock pulse energy over a data frame length of approximately 15 seconds. This digital value of SPA is then converted back into an analog voltage for comparison with limits in the decision circuitry.

Predetermined limits are stored in memory on the CPU limit storage board. The decision circuitry processes this information, and the results are sent to the display memory and driver board where it is stored in memory and displayed on the control panel. Simultaneously and End of Cycle (E.O.C.) signal is sent to the sequencer so that the next channel can be tested.

3.3.9 Sequencer (SEQ)

The Sequencer, under commands from the control panel and status input from the CPU, provides sequential control over the entire system and ensures that only one event occurs at a time. The control panel pushbuttons and the CPU status enables the sequencer to enter its various modes. The sequencer uses these modes to address and control the rest of the SPADE circuits for proper processing and display.

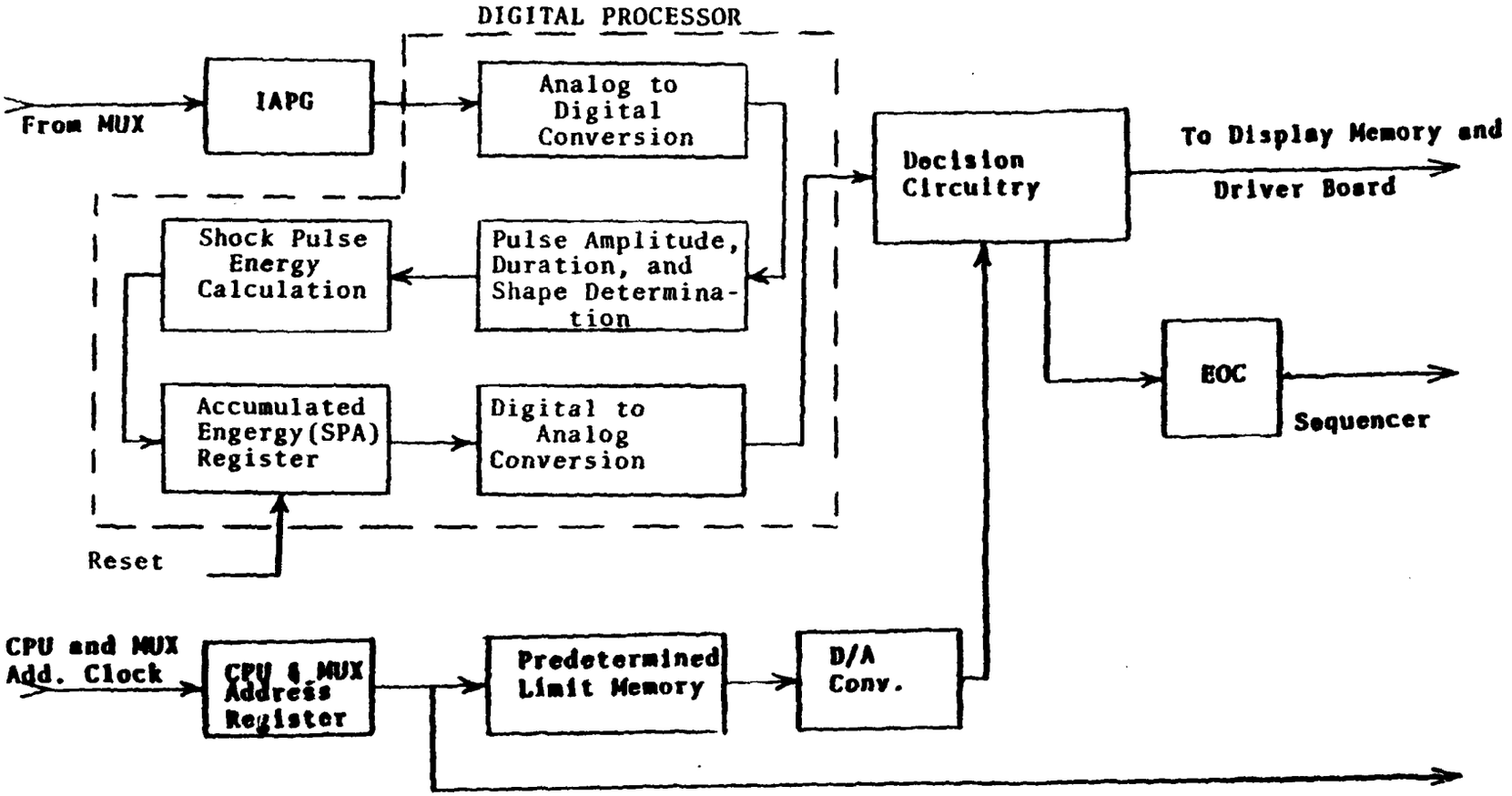

FIGURE 13 - CENTRAL PROCESSOR UNIT (CPU)

Functional Description

As referenced in Figure 14, the sequencer consists of RUN, ADVANCE, HOLD,and MONITOR Controls, an End of Cycle (EOC) recognition circuit, power on and timing sources, and signal routing to interconnect these functions and controls to the CPU and display memory.

The front panel control functions have switch debounce circuity for the different modes of operation. Each mode can be activated by depressing a pushbutton switch. The RUN mode is entered automatically by the power on initiation circuitry. It is terminated automatically by any non-pass condition. During the RUN mode, each input channel is processed sequentially, its result stored and displayed, and the next channel is processed. The ADVANCE mode causes the display memory to advance to the next channel allowing review of previously stored results. Constant depression of this switch, after a two second delay, will cause the channels to be sequenced at approximately a one half second rate. The MONITOR mode allows the same channel to be continuously processed by the CPU, with a display update after each CPU cycle.

The HOLD mode, when activated by either direct command at the control panel or automatically from the CPU, will terminate processing of information.

The EOC detect circuitry recognizes that the CPU has finished processing a channel of input data, issues a write command to store this newly processed data in memory, advances the CPU address on the CPU board to the next channel, and issues a trigger command to the CPU to begin a new processing cycle.

The timing source consists of a free running, astable multivibrator and a nine-stage binary divide down counter. A decoder

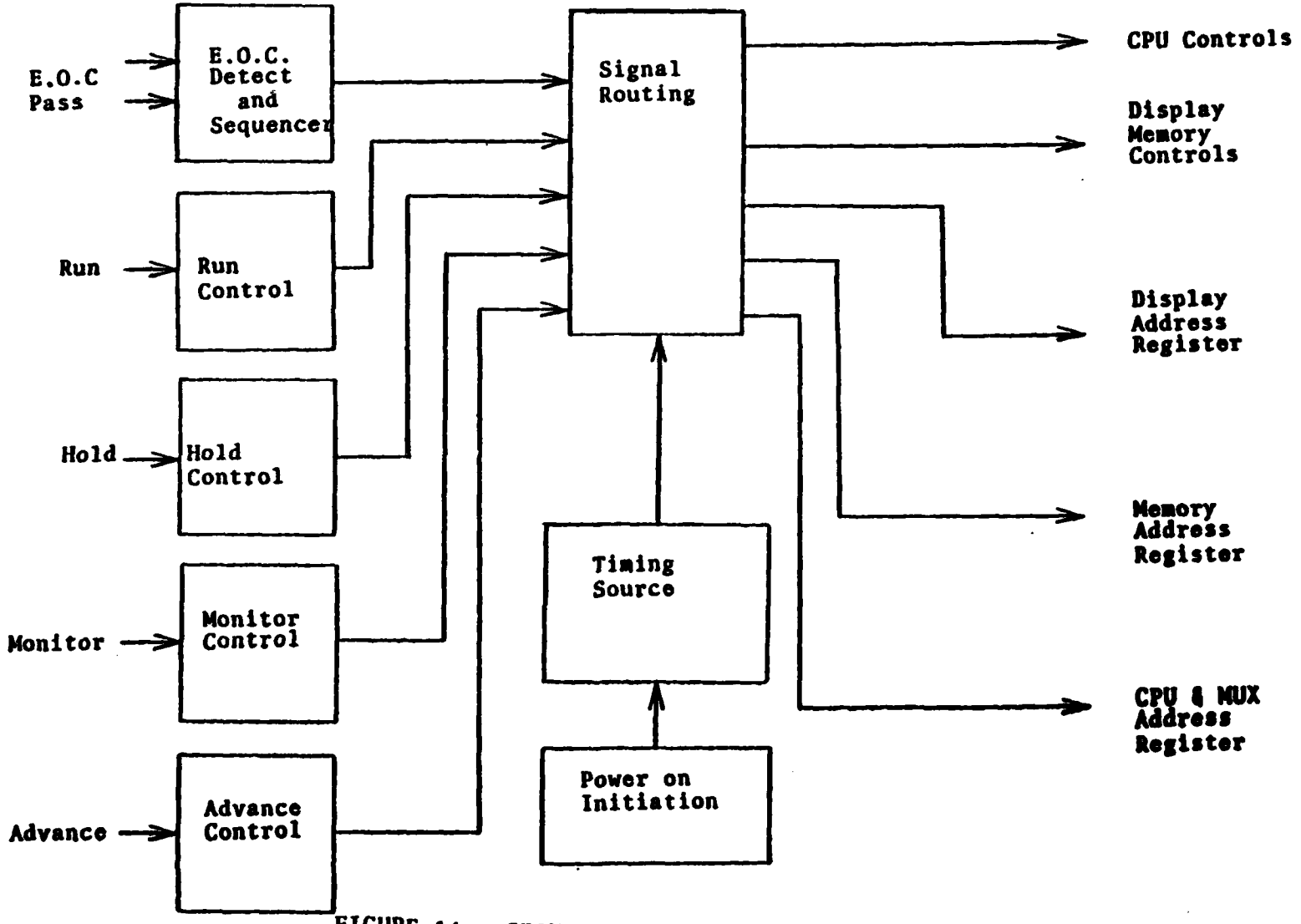

FIGURE 14 - SEQUENCER FUNCTIONAL BLOCK DIAGRAM

circuit establishes eight non-coinciding phases of the clock. This phased clocking allows the sequencer operations to occur in an orderly fashion and without race conditions. The final divide down output is a 1.6 HZ clock to enable blinking of the front panel channel display for enunciation.

The power initiation function detects the power turn-on conditions with an R-C charging circuit and causes an initiation cycle to begin. This cycle resets all controls, presents a CLEAR command to the memory while cycling its address and write function, resets all address registers to channel 0, enables the aircraft I.D. Code to be displayed in the channel position, and sets the RUN mode into operation for the STG reading into channel 0.

3.3.10 Display Memory & Drivers

The Display Memory and Drivers, as directed by the sequencer, store data from the CPU and display this data along with the channel location, on the control panel. The CPU data is converted to a percent limit value and the status of the particular channel is presented on control panel displays as well as entered into memory. The aircraft I.D. code is displayed at power turn on while all memories are being cleared.

Functional Description

The display memory and drivers as shown in Figure 15 consist of the display address register; the memory address register, the decoder drivers; a percent limit conversion and memory with decoder drivers; a status encoder, memory, decoder and indicator drivers; and a LIMIT SET encoder.

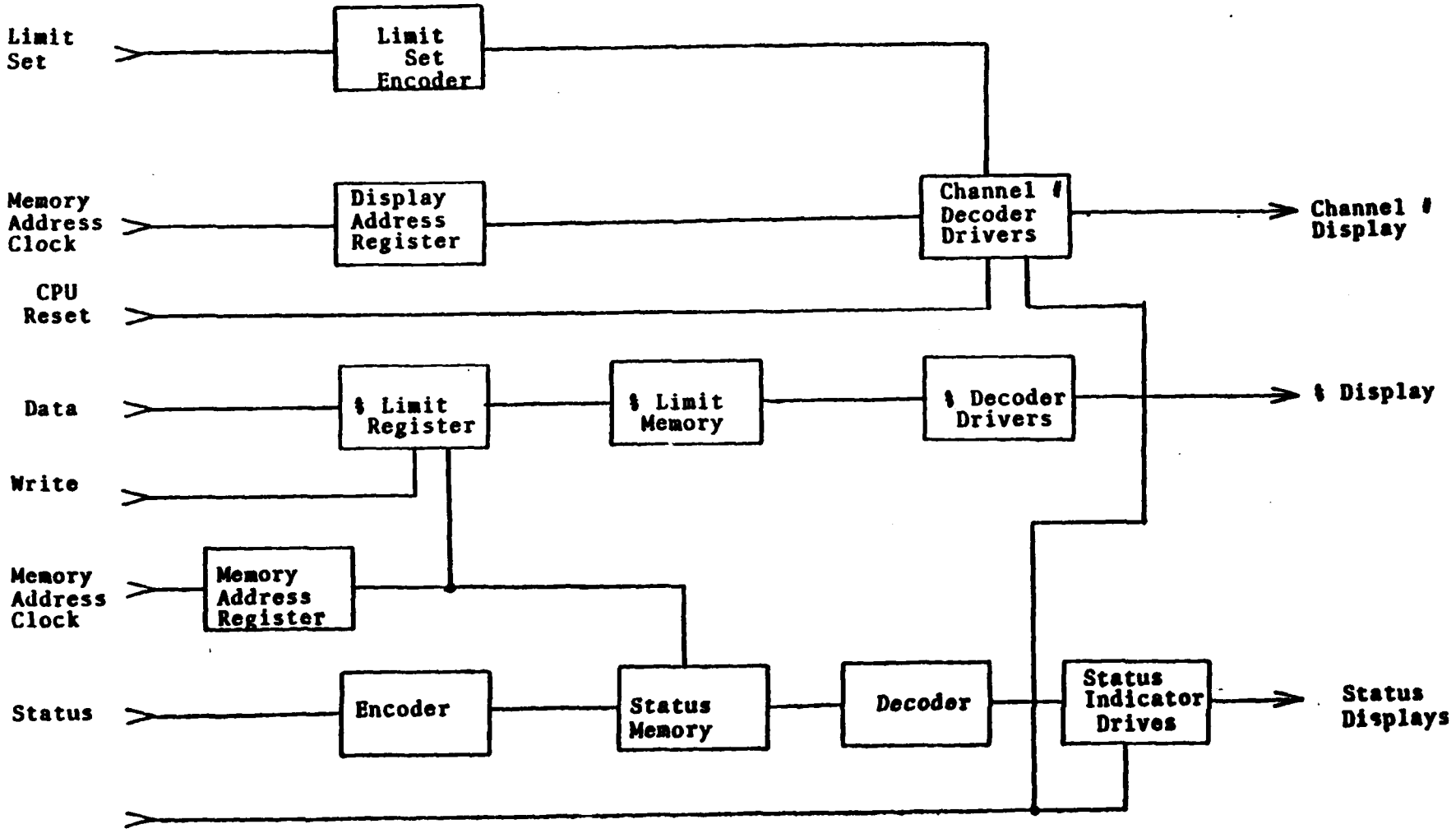

FIGURE 15 - DISPLAY MEMORY & DRIVERS FUNCTIONAL BLOCK DIAGRAM

The display address register and memory address register present the same address, the former in 2 BCD digits and the latter in a 5 bit binary code. These two registers enable the selected channel number and data to be displayed. The memory address also allows the proper write address after a CPU processing cycle.

The decoder drivers convert the two digit BCD channel address to seven segment digital outputs. The CPU reset and blink lines together enable the displayed channel digits to blink whenever new data is being processed in the CPU.

When applicable, the two digit percent limit is calculated and written into a 32 word 8 bit memory for indexing and display. Each percentage value, along with its associated channel number, is digitally displayed with light omitting diodes (LED) on the control panel.

The value shown will be the data of the channel displayed. The status lines from the CLS & CPU board and the clear function from the sequencer are decoded into a 4 bit word and stored in a 32 word by 4 bit memory. When the memory word is addressed, the output is presented to a decoder network to allow display of component condition using lamps which indicate good or servicable (green), caution (yellow) and remove or discrepant (red). Three additional red lights are used to indicate SENSOR OPEN, SELF TEST FAIL, and INPUT SATURATION.

The Aircraft I.D. Code is automatically displayed by the "Channel" LED's for a period of 5-6 seconds immediately after turning on power, and just prior to initiation of "SELF TEST" on Channel 00. The coding for this I.D. number is accomplished by permanent wiring inside the No. 1 Cannon Plug type connector of the sensor harness. Each aircraft type with its peculiar set of sensor locations has its own code. Memory capacity in SPADE limits the number of Aircraft I.D. Codes with associated limit sets to eight (8).

4.0 Contractor Evaluation - The contractor evaluation of the SPADE field prototype units included sensor and electronic unit circuit design refinements as well as preliminary definition and programming of test limits for "CAUTION" and "REMOVE" indications.

Testing was conducted on tail rotor driveshaft hanger bearings in the laboratory Bearing Test Fixture (BTF), on 42° gearboxes in a test cell, and on UH-1H & AH-1G aircraft at Ft. Rucker, Alabama. The data gathered from five (5) aircraft in "baseline" condition was used to develop generic baseline and warning threshold Shock Profile Area (SPA) values on the subject aircraft drive system components. (A "generic" baseline or warning threshold is a common valued limit for all serial number components with a common part number.) Data was also gathered from thirty-one (31) implanted defects on one UH-1H aircraft to verify that warning thresholds were not set too high. Finally, these emperically derived generic baselines and (yellow/red) warning thresholds were converted to Binary Coded Decimal (BCD) format and programmed into SPADE memory for use during government testing.

4.1 Circuit Design Refinements - The testing of the three SPADE field prototypes began with good and bad tail rotor driveshaft hanger bearings on the BTF in the laboratory. Although adequate diagnostic discrimination levels were achieved in this environment, higher background noise levels encountered during on-aircraft testing required modification of the IAPG section of the SPADE Electronic Unit. These changes involved redesign of the Band Pass Filter (BPF) to provide sharper roll-off characteristics and the incorporation of a new

Analog-to-Digital Conversion (ADC) circuit to provide greater fidelity in digitizing the envelope detected Shock Pulse signal. In addition, one Integrated Circuit (IC) chip in the Sequencer (SEQ) section was replaced when it became apparent that it did not consistantly behave as described in the manufacturer's specification. After these changes were accomplished, but before returning to on-aircraft testing, the SPADE with a redesigned Input Amplifier Pulse Generator (IAPG) was evaluated on a 42° gearbox in a test cell. During this testing, baseline values were obtained and followed by three separate implant conditions as shown in Figures 16 through 19 . Since the diagnostic discrimination ratios between implanted discrepant bearings and baseline bearings was good (ranging from approximately 3/1 to 20/1), the on-aircraft data collection effort at Ft. Rucker was resumed.

4.2 On-Aircraft Baseline and Implanted Defect Testing - Figure 20 shows the sensor locations and components monitored on a UH-1H helicopter. (Note that although engine bearings could have been monitored they were omitted due to the cost and schedule impact of accomplishing engine bearing implant tests.) The only difference between the UH-1H and AH-1G in these tests was that one less sensor location was involved due to there being one less tail rotor driveshaft hanger bearing. All other drive system components in these two aircraft models have the same part numbers and are therefore diagnosed by the same generic baseline and warning threshold criteria. Tables III through XII summarize the data collected during this phase of the Contractor Evaluation.

4.2.1 Each of these SPADE Contractor Evaluation Data tables pertains to a given sensor location, such as "UH-1H Transmission Input Pinion". All data for a given sensor location is divided into two categories: "Baseline Data" and "Implant Data". Each of these categories

(TEXT continues on page 65.)

42° Gearbox S/N ABB1560
Speed - 4700 RPM

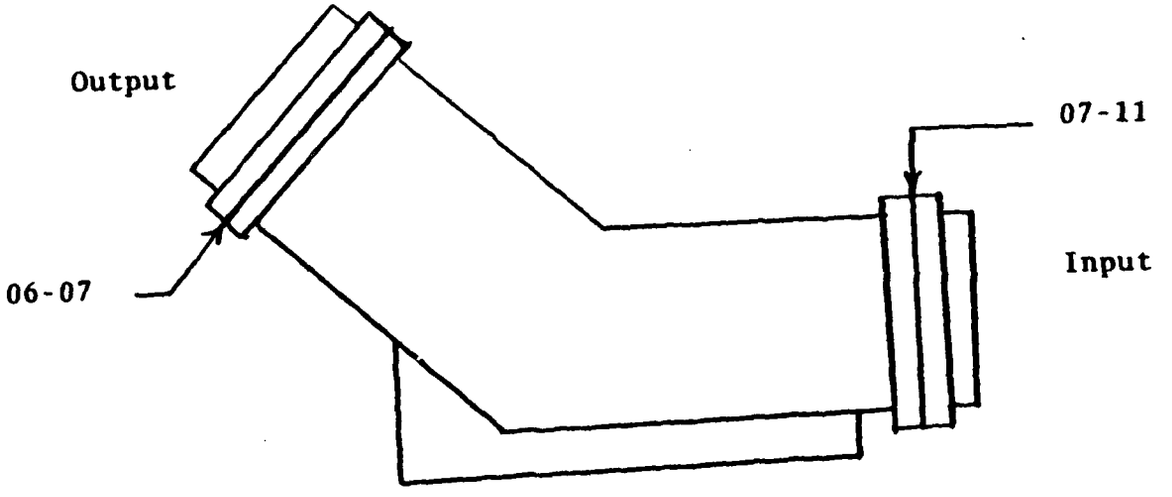

FIGURE 16-42° Gearbox Baseline SPADE Readings (Test Cell Data)

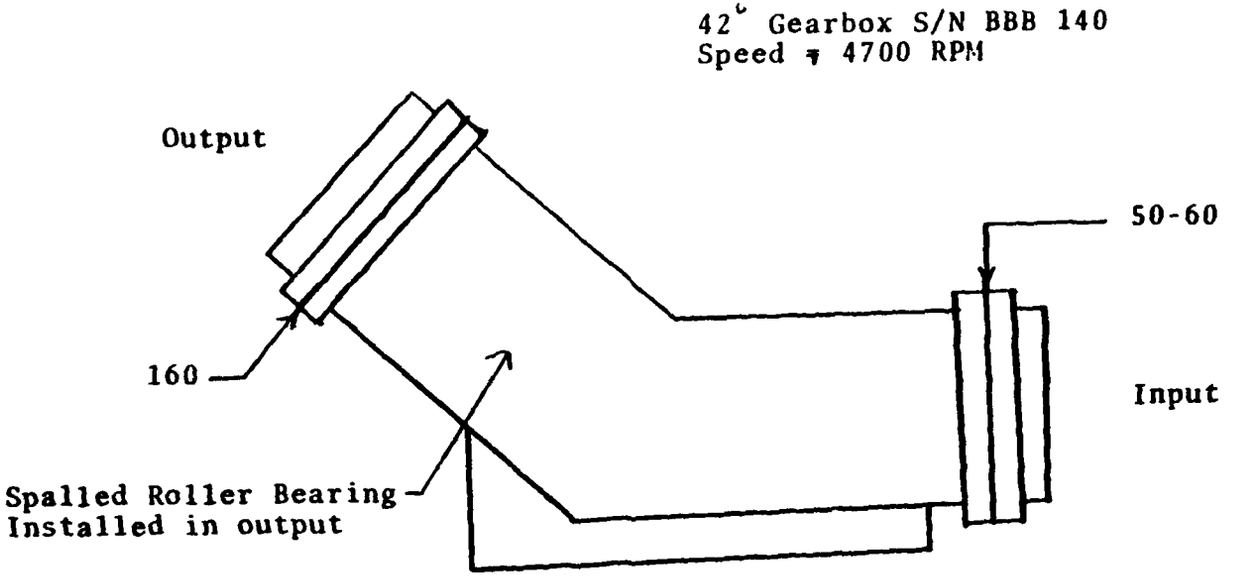

FIGURE 17 - 42° GEARBOX IMPLANT BHC-021 SPADE READINGS (TEST CELL)

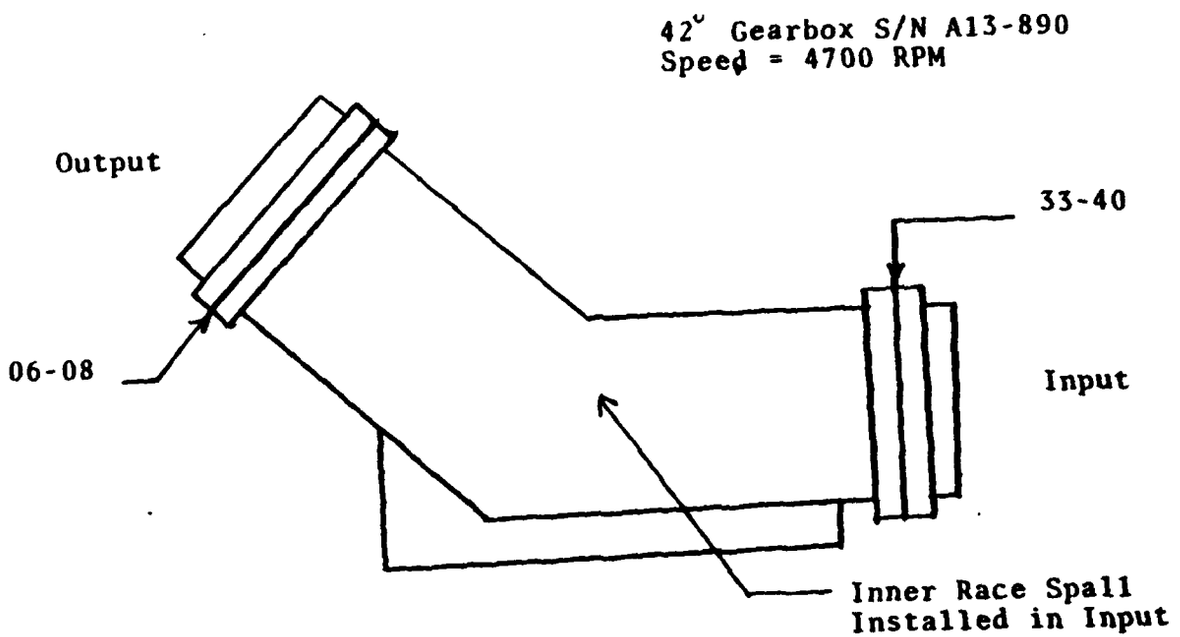

FIGURE 18 - 42° GEARBOX IMPLANT MAIC 003 SPADE READINGS (TEST CELL)

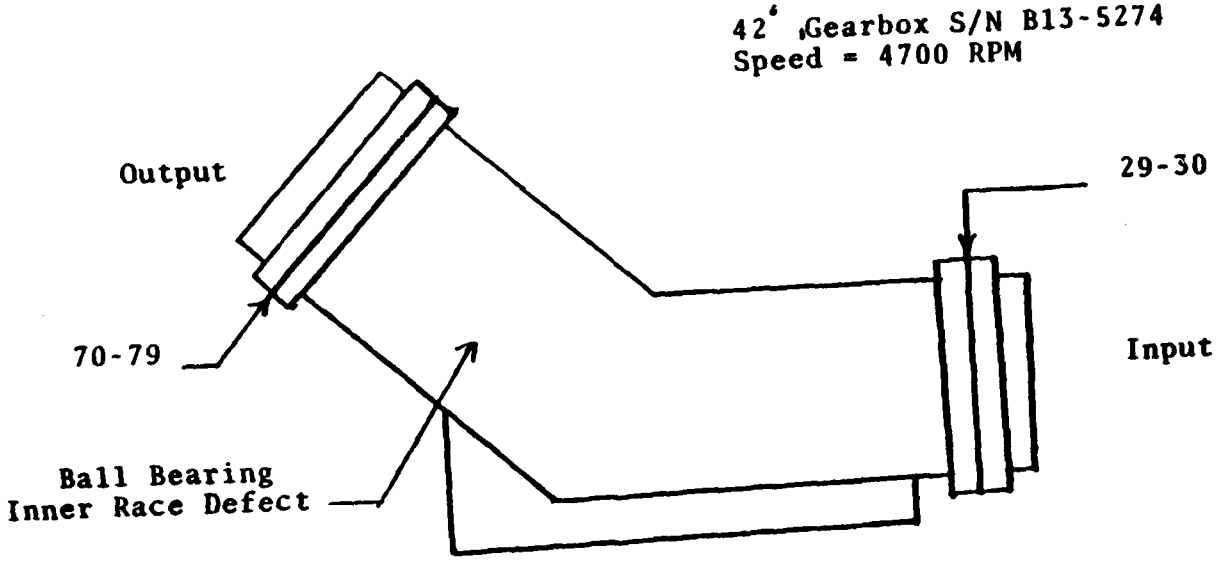

FIGURE 19 - 42° GEARBOX IMPLANT MAIC - 011 SPADE READINGS (TEST CELL)

1 - Transmission Input Pinion

2 - Transmission Upper Mast Bearing

3 - Tailrotor Drive Quill

4 - 42° Gearbox Input Pinion

5 - 42° Gearbox Output Pinion

6 - 90° Gearbox

7 - #1 Hanger Bearing

8 - #3 Hanger Bearing

9 - #4 Hanger Bearing

10 - #2 Hanger Bearing

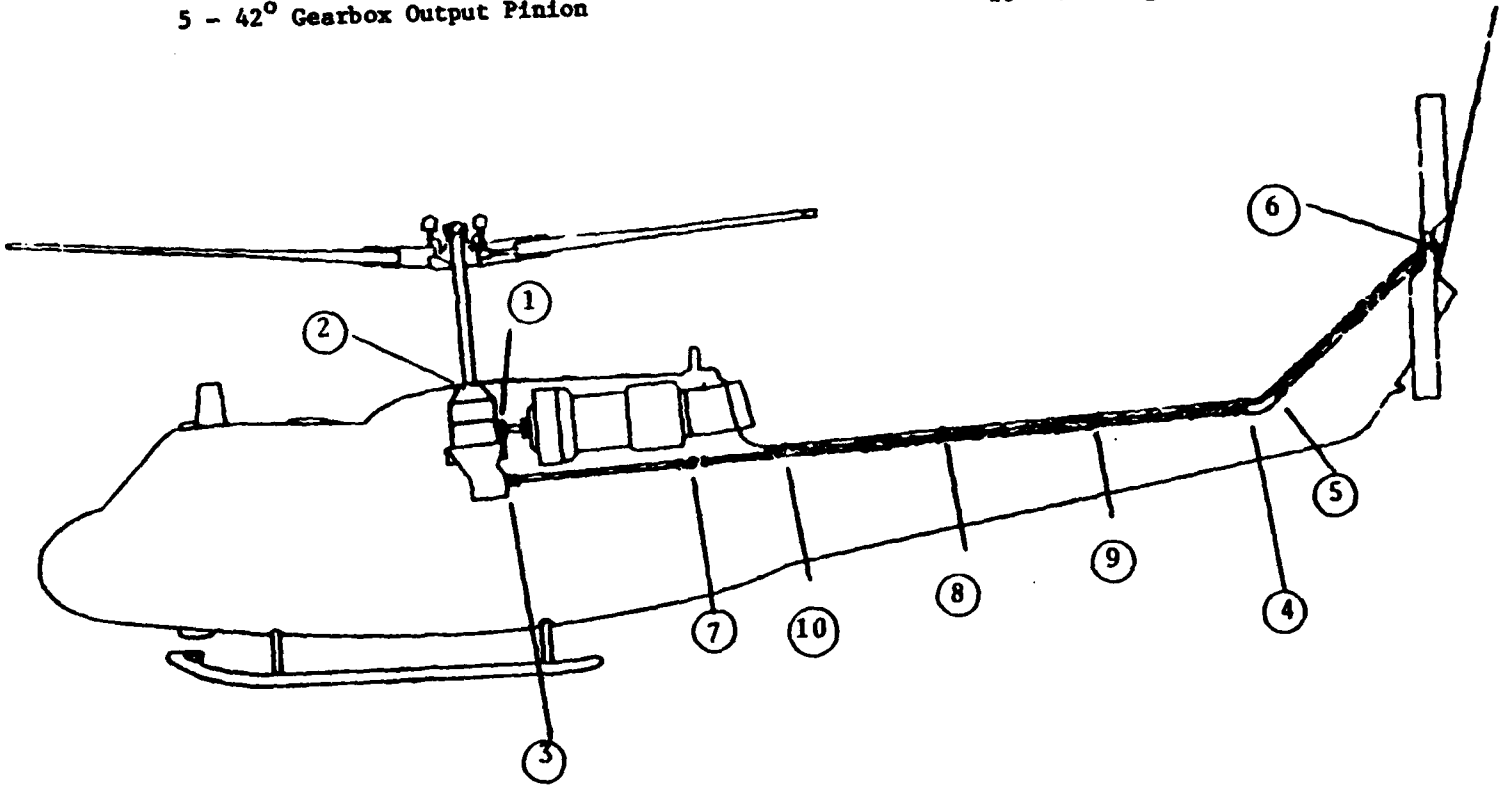

FIGURE 20 - UH-IH COMPONENTS & SENSOR LOCATIONS

TABLE III

SPADE Contractor Evaluation Data

UH-1H Transmission Input Pinion

BASELINE DATA				IMPLANT DATA				
A/C #	Run #	Endevco or B & K	BB & N	Implant #	Run #	Endevco or B & K	BB & N	SPADE #
BC-13	26-B	17		BHC-093	34-I	415-503		001
	30-B	30-33			41-I	347-350		
	31-B	30-32			42-I	305-309		
	36-B	34-35			47-I	193-203		
	37-B	37		BHC-012	53-I		54	
	48-B	35-55 (Lube contamination?)			54-I		62-69	
					55-I	9-10		
	52-B			MAIC-025	58-I	75		
	56-B		168-172		59-I		315-324	
	57-B	8-9			61-I		281	
	62-B		70-74	BHC-081	63-I	06		
	65-B	05-06		BHC-081	64-I		167-170	
	66-B		366-375	MAIC-018	70-I	09-11		
BC-15	39-B	24		MAIC-018	71-I		49	
BC-6	43-B	50-58 (Baseline?)						
BC-10	67-B	25-26						
BC-25	68-B		102-103					
BC-25	69-B	10						

Note: Calculated values include all data from SPADE units 001 & 002

$\bar{x}$ = 23.5 σ = 11.2
Range = 05-37

$\bar{x} + \sigma$ = 34.7
$\bar{x} + 2\sigma$ = 45.9
$\bar{x} + 3\sigma$ = 57.1

* Limit Set #1 (M3 Sensors)	*Limit Set #2 (M2 Sensors)
Yellow = 54.5	Yellow = 41.3
Red = 82.9	Red = 62.8

* See Figure 21 for definition of limit calculation procedures

TABLE - III (cont'd)

SPADE Contractor Evaluation Data

UH-1H Transmission Input Pinion

BASELINE DATA				IMPLANT DATA				
A/C #	Run #	Endevco or B & K	BB & N	Implant #	Run #	Endevco or B & K	BB & N	SPADE #
BC-13	62-B		69-73	BHC-081	63-I	06		002
BC-13	65-B	06		BHC-081	64-I		147-149	
BC-10	60-B	01		MAIC-018	70-I	12-13		
BC-10	66-B		378-384	MAIC-018	71-I		24-27	
BC-10	67-B	34						

Note: Calculated values include all data from SPADE units 001 & 002

$\bar{x}$ = 23.5 σ = 11.2
Range = 05-37

$\bar{x} + \sigma$ = 34.7
$\bar{x} + 2\sigma$ = 45.9
$\bar{x} + 3\sigma$ = 57.1

Limit Set #1 (M3 Sensors)	Limit Set #2 (M2 Sensors)
Yellow = 54.5	Yellow = 41.3
Red = 82.9	Red = 62.8

TABLE IV

SPADE Contractor Evaluation Data
UH-1H Transmission Mast Bearing

BASELINE DATA				IMPLANT DATA				
A/C #	Run #	Endevco or B & K	BB & N	Implant #	Run #	Endevco or B & K	BB & N	SPADE #
BC-13	26-B	21-22		BHC-124	54-I		110-112	001
	36-B	15-17			55-I	13-14		
	37-B	19-20			58-I	4-13		
	56-B		98-124		59-I		36-50	
	62-B		70-74		61-I		51	
	66-B		70-71	BHC-132	63-I	11		
BC-15	39-B	16		BHC-132	64-I		62-63	
BC-6	43-B	13-15		SKF-025	70-I	106		
BC-10	67-B	13-14		SKF-025	71-I		37-38	
BC-13	62-B		116-120	BHC-132	63-I	11		002
BC-13	66-B		191-209	BHC-132	64-I		64-68	
BC-10	67-B	14-16		SKF-025	70-I	96		
				SKF-025	71-I		89-91 (loose sensor)	

CALCULATED DATA

$\bar{x}$ = 16.8 σ = 3.2
Range = 13-22

$\bar{x} + \sigma$ = 20.0
$\bar{x} + 2\sigma$ = 23.2
$\bar{x} + 3\sigma$ = 26.4

Limit Set #1 (M3 Sensors)

Yellow = 27.8

Red = 38.6

Limit Set #2 (M2 Sensors)

Yellow = 20.9

Red = 29.0

Table V

SPADE Contractor Evaluation Data

UH-1H Transmission Tailrotor Drive Quill

BASELINE DATA				IMPLANT DATA				
A/C #	Run #	Endevco or B & K	BB & N	Implant #	Run #	Endevco or B & K	BB & N	SPADE #
BC-13	26-B	14		BHC-023	28-I	232-233		001
	30-B	14-17		BHC-023	29-I	175		
	31-B	14-16		BHC-008	63-I	35-37		
	36-B	24-27		BHC-008	64-I		109-114	
	37-B	22-28		MAIC-009	70-I	25		
	56-B		68-83	MAIC-009	71-I		09	
	57-B	21						
	62-B		19-20					
	65-B	12-13						
	66-B		180-190					
BC-15	39-B	24						
BC-6	43-B	12-13						
BC-10	60-B	20-32						
BC-10	67-B	21-22						
BC-13	65-B	12-13		BHC-008	63-I	35-37		002
BC-10	66-B		156-174	BHC-008	64-I		102-109	
BC-10	67-B	22-23		MAIC-009	70-I	30-32		
				MAIC-009	71-I		20-21	

$\bar{x}$ = 19.3 σ = 6.0
Range = 14-32

$\bar{x} + \sigma$ = 25.3
$\bar{x} + 2\sigma$ = 31.3
$\bar{x} + 3\sigma$ = 37.3

Limit Set #1 (M3 Sensors)

Yellow = 27.6

Red = 40.2

Limit Set #2 (M2 Sensors)

Yellow = 28.2

Red = 41.0

TABLE VI
SPADE Contractor Evaluation Data

UH-1H No. 1 Hanger Bearing

BASELINE DATA				IMPLANT DATA				
A/C #	Run #	Endevco or B & K	BB & N	Implant #	Run #	Endevco or B & K	BB & N	SPADE #
BC-13	26-B	199-200 (new brng., 1st run)		SKF-001	28-I	843-850		001
	30-B	89-93		SKF-001	29-I	1655		
	31-B	74-76		SKF-005	41-I	419-924		
	36-B	01 (connect.fail?)			42-I	130-135		
	56-B		133-135		46-I	139-143	471-968	
	57-B	16-17			54-I			
	62-B		119-122		55-I	197-202		
	65-B	17		SKF-023	58-I	323-330		
BC-6	43-B	51-52			59-I		990-1022	
BC-10	66-B		1848-1859 (B/L??)		61-I		769	
BC-10	67-B	581-589 (B/L??)			63-I	424-429		
					64-I		819-829	
					70-I	919-924		
					71-I		118-121	
BC-13	62-B		198-199	SKF-023	63-I	460-474		002
BC-13	65-B	16-18			64-I		949-967	
BC-10	66-B		1929-1987 (B/L??)		70-I	919-924		
BC-10	67-B	707-720 (B/L??)			71-I		118-121	

$\bar{x}$ = 80.4 σ = 65.2
Range = 16-200

$\bar{x} + \sigma$ = 145.6
$\bar{x} + 2\sigma$ = 210.8
$\bar{x} + 3\sigma$ = 276.0

Limit Set #1 (M3 Sensors)

Yellow = 201.1

Red = 321.8

Limit Set #2 (M2 Sensors)

Yellow = 189.7

Red = 303.6

Table VII

SPADE Contractor Evaluation Data

UH-1H No. 2 Hanger Bearing

BASELINE DATA				IMPLANT DATA				
A/C #	Run #	Endevco or B & K	BB & N	Implant #	Run #	Endevco or B & K	BB & N	SPADE #
BC-13	26-B	168-169 (new brng)		SKF-002	28-I	885-1006		001
	30-B	05-08		SKF-002	29-I	728		
	31-B	05		SKF-024	58-I	109-116		
	36-B	03-06			59-I		314-324	
	37-B	05-12 (couplant)			61-I		317	
	56-B		172-188		63-I	90		
	57-B	99-117			70-I	171-174		
	62-B		240-249		71-I		16-17	
	65-B	88-107						
BC-15	39-B	35						
BC-6	43-B	19-20						
BC-10	60-B	245-262 (B/L??)						
	66-B		350-363 (B/L??)					
	67-B	436-462						
BC-13	62-B		204-226	SKF-024	63-I	84-100		002
BC-13	65-B	123-137			64-I		417-432	
BC-10	66-B		371-383 (B/L??)		70-I	199-200		
BC-10	67-B	699-682 (B/L??)			71-I		17-18	

$\bar{x}$ = 54.1 σ = 60.5

Range = 5-169

	Limit Set #1 (M3 Sensors)	Limit Set #2 (M2 Sensors)
$\bar{x} + \sigma$ = 114.6	Yellow = 222.2	Yellow = 157.6
$\bar{x} + 2\sigma$ = 175.1		
$\bar{x} + 3\sigma$ = 235.6	Red = 365.4	Red = 259.2

Table VIII

SPADE Contractor Evaluation Data

UH-1H No. 3 Hanger Bearing

BASELINE DATA				IMPLANT DATA				
A/C #	Run #	Endevco or B & K	BB & N	Implant #	Run #	Endevco or B & K	BB & N	SPADE #
BC-13	26-B	01-02 (new brng, bad cable)		SKF-003	28-I	02 (bad cable)		001
	36-B	55-57		EKF-003	29-I	07 (bad cable)		
	37-B	42-43 (couplant)		SKF-001	41-I	135-139 (loose pad)		
	56-B		379-387		42-I	616-675		
	57-B	128-133			46-I	1180-1250		
	62-B		649-657		47-I	1060-1238		
	65-B	239-246 (B/L??)			54-I		1978-2122	
BC-6	43-B	23-25			55-I	1380-1509		
BC-10	60-B	24-50			58-I	1199-1258		
	66-B		09-11		59-I		1734-2059	
	67-B	23-25			61-I		1516-1539	
					63-I	1590-1620		
					64-I		2306-2335	
					70-I	848-874		
					71-I		1060-1082	
BC-13	62-B		690-718	SKF-001	63-I	1618-1787		002
BC-13	65-B	272-273			64-I		2350-2364	
BC-10	66-B		06-08		70-I	880-884		
BC-10	67-B	30-39			71-I		1050-1102	

$\bar{x}$ = 52.3 σ = 34.0
Range = 23-133

$\bar{x} + \sigma$ = 86.3
$\bar{x} + 2\sigma$ = 120.3
$\bar{x} + 3\sigma$ = 154.3

Limit Set # 1
(M2 Sensors)

Yellow = 114.8

Red = 179.9

Limit Set #2
(M2 Sensors)

Yellow = 108.3

Red = 169.7

TABLE IX

SPADE Contractor Evaluation Data

UH-1H No. 4 Hanger Bearing

BASELINE DATA				IMPLANT DATA				
A/C #	Run #	Endevco or B & K	BB & N	Implant #	Run #	Endevco or B & K	BB & N	SPADE #
BC-13	26-B	150-152 (new brng)		SKF-004	28-I'	08		001
	30-B	17-19		SKF-004	29-I	10-110		
	31-B	26-27		SKF-002	41-I	26-29		
	36-B	21-23			42-I	226-228		
	37-B	0-44 (couplant)			46-I	239-257		
	56-B		25-28		47-I	260-374		
	57-B	08-09			54-I		249-253	
	65-B	08-11			55-I	305-309		
BC-6	43-B	62-75			58-I	314-320		
BC-10	66-B		495-496(B/L??)		59-I		223-231	
BC-10	67-B	570-575 (B/L??)			61-I		122	
					63-I	354-405		
					64-I		160	
					70-I	189-194		
					71-I		231-236	
BC-13	65-B	07		SKF-002	63-I	404-436		002
BC-10	66-B		432-482(B/L??		64-I		160-163	
BC-10	67-B	574-647 (B/L??)			70-I	181-184		
					71-I		292-302	

$\bar{x}$ = 43.5 σ = 47.8
Range = 8-152

$\bar{x} + \sigma$ = 91.3
$\bar{x} + 2\sigma$ = 186.9
$\bar{x} + 3\sigma$ = 234.7

Limit Set #1 (M3 Sensors)

Yellow = 171.6

Red = 263.3

Limit Set #2 (M2 Sensors)

Yellow = 168.2

Red = 258.2

TABLE X

SPADE Contractor Evaluation Data

UH-1H 42° Gearbox Input Pinion

BASELINE DATA				IMPLANT DATA				
A/C#	Run#	Endevco or B & K	BB & N	Implant #	Run#	Endevco or B & K	BB & N	SPADE
BC-13	26-B	08-09		BHC-001	29-I	46		001
	30-B	10-11		BHC-001	34-I	33-36		
	31-B	08		MAIC-001	41-I	26-28		
	36-B	06-07			42-I	56		
	37-B	09-20 (couplant?)			46-I	05		
	56-B		31-34 (bad ground?)		47-I	07-15		
	62-B		21-23	MAIC-009	54-I		62-69	
	65-B	03		MAIC-009	55-I	34-38		
BC-15	39-B	15		MAIC-008	71-I		1274-1315	
BC-6	43-B	15-16						
BC-10	66-B		03-05					
BC-10	67-B	12-13						
BC-13	62-B		25-26	MAIC-008	71-I		1124-1132	002
BC-13	65-B	03-04						
BC-10	66-B		70-74					
BC-10	67-B	12-13						

$\bar{x}$ = 10.8 σ = 4.4
Range = 3-20

$\bar{x} + \sigma$ = 15.2
$\bar{x} + 2\sigma$ = 19.6
$\bar{x} + 3\sigma$ = 24.0

Limit Set #1 (M3 Sensors)

Yellow = 17.1

Red = 25.6

Limit Set #2 (M2 Sensors)

Yellow = 17.6

Red = 26.4

TABLE XI

SPADE Contractor Evaluation Data

UH-1H 42° Gearbox Output

BASELINE DATA				IMPLANT DATA				
A/C #	Run #	Endevco or B & K	BB & N	Implant #	Run #	Endevco or B & K	BB & N	SPADE #
BC-13	30-B	13-14		BHC-013	58-I	31		001
	31-B	12-13		BHC-013	59-I		48-50	
	36-B	12-13		BHC-013	61-I		26-34	
	37-B	12-15 (couplant?)		MAIC-010	63-I	72-74		
	56-B		47-50 (bad ground?)	MAIC-010	64-I		85-93	
				MAIC-001	70-I	55-56		
	57-B	7-8		MAIC-001	71-I		365-368	
	62-B		114-120					
	65-B	8-9						
BC-15	39-B	14						
BC-6	43-B	17-19						
BC-10	60-B	5-11						
BC-10	66-B		275-279					
BC-10	67-B	12						
BC-13	62-B		137-138	MAIC-010	63-I	79-82		002
BC-13	65-B	9-11		MAIC-010	64-I		87-91	
BC-10	66-B		315-319	MAIC-001	70-I	66-69		
BC-10	67-B	11-12		MAIC-001	71-I	40-41		

$\bar{x}$ = 11.9 σ = 3.5
Range = 5-19

$\bar{x} + \sigma$ = 15.4
$\bar{x} + 2\sigma$ = 18.9
$\bar{x} + 3\sigma$ = 22.4

Limit Set #1 (M3 Sensors)

Yellow = 18.5

Red = 26.9

Limit Set #2 (M2 Sensors)

Yellow = 17.0

Red = 24.6

TABLE XII

SPADE Contractor Evaluation Data

UH-1H 90° Gearbox

BASELINE DATA				IMPLANT DATA				
A/C #	Run #	Endevco or B & K	BB & N	Implant #	Run #	Endevco or B & K	BB & N	SPADE #
BC-13	30-B	02-03		BHC-025	28-I	66		001
	31-B	03		BHC-026	29-I	28 (loose pad)		
	36-B	04-05		BHC-031	34-I	39-42		
	37-B	03-04 (couplant)			41-I	39-40		
	56-B		25-29		42-I	49-51		
	57-B	03-04			46-I	28-30		
	62-B		15-16		47-I	29-35		
	65-B	11		MAIC-014	54-I		11-19	
BC-15	39-B	08			55-I	11-14 (bad ground?)		
BC-6	43-B	39-47 (B/L??)			58-I	06-07		
BC-10	66-B		07-08		59-I		04-06	
BC-10	67-B	09-11			61-I		08-13	
				BHC-099	63-I	12-14		
				BHC-099	64-I		14-15	
				BHC-091	70-I			
				BHC-091	71-I		22-24	
BC-13	62-B		08-10	BHC-099	63-I	14	15-17	002
BC-13	65-B	08-10		BHC-099	64-I			
BC-10	66-B		04-05	BHC-091	70-I	10-11		
BC-10	67-B	10-11		BHC-091	71-B		loose sensor	

$\bar{x}$ = 5.4 σ = 3.2

Range = 2-11

$\bar{x} + \sigma$ = 8.6

$\bar{x} + 2\sigma$ = 11.8

$\bar{x} + 3\sigma$ = 15.0

Limit Set #1 (M3 Sensors)

Yellow = 10.3

Red = 16.0

Limit Set #2 (M2 Sensors)

Yellow = 10.6

Red = 16.5

is further subdivided according to the type of sensor employed. The Endevco and B & K sensors were built to the same specification and are therefore considered as one sensor type referred to in the limit calculations as "M2" type sensors. The BB & N sensors were built to a slightly different specification which was intended to define a low cost sensor that could be cost effective as a permanently installed unit. However, the BB & N sensors showed unacceptably high sensor-to-sensor variability in readings taken on the same bearing and were therefore not used in determining baseline and warning threshhold values. The causes of this problem and the consequences in relation to future development of low cost sensors are discussed more fully in Section 5 of this report. The limit set for "M3" sensors on each of the Contractor Evaluation Data tables refers to the "ruggedized" type of sensor that was employed during FDTE. These M3 sensors were derivatives of the Endevco "M2" sensors but with slightly higher sensitivity and a more rugged BNC type electrical connector.

It should be noted that some of the components tested on the five (5) aircraft that were supposed to be in baseline (non-discrepant) condition were, in fact, found to be defective. These data are so indicated in Tables III through XII by parenthetic notes and were confirmed by spectral analysis of the shock pulse train and by teardown inspection. For example, referring to Table IX for the No. 4 Hanger Bearing position it can be seen that the Bearcat Ten (BC-10) aircraft had a very high SPADE reading (all SPADE readings on these tables are in absolute value terms). This bearing was subsequently removed, confirmed as defective and reused for implant tests. It's reading was therefore not included in the range of baseline values employed for

limit calculations.

One other important observation that came from the baseline testing is that the grease lubricated tail rotor driveshaft hanger bearings have rather high readings when first installed but that these readings decrease rapidly to normal values during the first few hours of operation. It is believed that this decrease in SPADE readings also indicates decreasing levels of friction as the grease becomes evenly distributed by initial operation of the bearing. A related observation of SPADE's ability to indicate lubrication effectiveness by detecting frictional energy was observed during the FDTE at Ft. Hood. It was found that if an oil lubricated gearbox had gradually increasing SPADE readings and was flushed with fresh oil, the readings after flushing would drop significantly and sometimes change the SPADE indication from yellow (CAUTION) back down to green (GOOD).

4.2.2 All testing of components with implanted defective bearings was accomplished on one aircraft, Bearcat 14. During this portion of the Contractor Evaluation Testing, a total of thirty-one (31) implant configurations were tested. Twenty-four (24) of these implant configurations were detectable by abnormally high SPADE readings but seven (7) produced measured levels of kinetic and frictional energy that were within normal baseline limits. Table XIII is a summary of these test results which describes the implant configurations and identifies each as either a "HIT" (correctly diagnosed defect) or a "MISS" (undetected implant). Some of the "misses" may have been due to variations in sensor sensitivity but this is not believed to be the principle cause. The primary reason that some implant configurations were not detected is believed to be related to the disassembly and

TABLE XIII

SPADE UH-1H

Implant Test Bearings

"HITS"

BHC-093

.Ball bearing inner race spall

.Xmsn input pinion

-4 tests, 4 hits (all red lights)

MAIC-025

.Ball bearing inner race spall

.Xmsn input pinion

-1 test, 1 hit (red light)

SKF-025

.Ball bearing inner race, outer race, and ball spalls
.Xmsn Mast Bearing

- 2 tests, 2 hits (red lights)

BHC-023

.Roller bearing inner race spall

.Tail rotor drive quill (main Xmsn)

- 2 tests, 2 hits (red lights)

BHC-008

.Ball bearing outer race spall

Tail rotor drive quill (main Xmsn)

-2 tests, 2 hits (yellow lights @ 61%)

MAIC-009

.Roller bearing inner race spall

.Tail rotor drive quill (main Xmsn)

-2 tests, 1 hit (yellow @ 22%) & 1 miss

.42° Gearbox Input Pinion

-1 test, 1 hit (red light)

HITS (contd)

BHC-001

.Ball bearing outer race spall

.42° Gearbox Input Pinion

- 2 tests, 2 hits (Red lights)

MAIC-011

.Ball bearing inner race spall

.42° Gearbox Input Pinion

- 4 tests, 2 hits (Red lights) & 2 misses

BHC-013

.Roller bearing inner race spall

.42° Gearbox Output Pinion

- 1 test, 1 hit (Red light)

MAIC-010

.Ball bearing ball spall

.42° Gearbox Output Pinion

- 2 tests, 2 hits (Red lights)

MAIC-001

.Ball bearing ball spall

.42° Gearbox Output Pinion

-2 tests, 2 hits (Red lights)

BHC-025

.Roller bearing roller spall

.90° Gearbox

- 2 tests, 2 hits (red lights)

BHC-031

.Roller bearing roller spall

.90° Gearbox

- 5 tests, 5 hits (red lights)

"HITS"(Cont'd)

MAIC-014

.Ball bearing inner race spall

.90° Gearbox

- 2 tests, 1 hit (yellow light @ 49%) & 1 miss

BHC-099

.Roller bearing, roller spall

.90° Gearbox

- 2 tests, 2 hits (yellow lights @58%)

BHC-091

.Ball bearing outer race spall

.90° Gearbox

-2 tests, 2 borderline hits (yellow lights @ 7%)

SKF-002

.Ball bearing (Discrepancy unknown)

.Tail rotor driveshaft #4 hanger bearing

-10 tests, 9 hits & 1 miss:

(4 yellow lights @ 14% to 99%)

(5 red lights)

.Tail rotor driveshaft #2 hanger bearing

-2 tests, 2 hits (red lights)

SKF-001

.Ball bearing (discrepancy unknown)

.Tail rotor driveshaft #1 hanger bearing

-2 tests, 2 hits (red lights)

.Tail rotor driveshaft #3 hanger bearing

-10 tests, 10 hits (9 red + 1 yellow @ 47%)

SKF-024

.Ball Bearing (discrepancy unknown)
.Tail rotor driveshaft #2 hanger bearing

- 5 tests, 2 hits (yellow 15% to 41%) & 3 misses

SKF-005

.Ball bearing inner race spall (artificial)

.Tail rotor drive shaft #1 hanger bearing

-4 tests, 2 hits & 2 misses:

(1 yellow light @9%)

(1 red light)

SKF-023

.Ball bearing (discrepancy unknown)

.Tail rotor driveshaft #1 hanger bearing

-5 tests, 5 hits (red lights)

(Note: Some of the above bearings were implant tested in more than one configuration) TOTAL MISSES

BHC-012

.Roller bearing inner race spall

.Xmsn Input Pinion

-1 miss

BHC-081

.Ball bearing outer race spall

.Xmsn Input Pinion

-2 misses

MAIC-018

.Ball bearing inner race spall

.Xmsn Input Pinion

-2 misses

BHC-124

.Ball bearing outer race spall

.Xmsn Mast Bearing

-2 misses

TOTAL MISSES (cont'd)

BHC-132

.Ball bearing outer race spall

.Xmsn Mast bearing

-2 misses

SKF-004

.Ball bearing with moderate corrosion on balls & races

.Tail rotor driveshaft #4 hanger bearing

-2 misses

SKF-003

.Ball bearing with light corrosion on both races

.Tail rotor driveshaft #3 hanger bearing

-2 misses

reassembly of components during the implant build-up process. Since the defective bearings were removed from one gearbox or bearing housing and reinstalled into another without knowing the geometry of the defect relative to the bearing load zone in its "native" (where it became discrepant) component, there is no way to know if the reassembled implant configuration in an "alien" component would cause similar levels of kinetic and frictional energy release. This uncertainty about the dynamic similarity between native and implant configurations is further confused by the fact that many of the bearings were disassembled and cleaned prior to reinstallation as an implant. This means that trapped debris particles associated with the discrepant bearing in its native environment were not present in the implant configuration, which would certainly result in lower SPADE readings. In support of this hypothesis, it should be noted that at each sensor location where a miss occurred, one or more hits were achieved during this same series of implant tests. These implant test results will be discussed further in Section 4.4.1 on SPADE accuracy.

4.3 SPADE Limit Calculations - The limits employed during the FDTE were based upon SPADE readings obtained from baseline UH-1H components during the Contractor Evaluation. Due to the limited population of components tested, these limits are considered to be preliminary only, and, though adequate for initial field testing, should be revised based upon field experience prior to fleetwide application.

Actually two different sets of limits were calculated and programmed into the SPADE units for use during FDTE. The first set of limits was tailored to the M2 type of sensors that were used during the Contractor Evaluation and the early portion of the FDTE at Ft. Hood. The second set of limits was for use with the M3 type sensors

which did not become available until after the FDTE began. The M3 sensor limits had to be programed into SPADE memory prior to the availability of any M3 sensors, in order to not delay or interrupt the FDTE. Therefore, the limits calculated for use with M2 sensors were modified by two factors; one to account for the sensitivity difference between M2 and M3 sensors, and the other to allow for a projected ± 10% tolerance in readings between individual M3 type sensors.

Figure 21 outlines the procedure used to calculate the yellow (caution) and red (remove) SPADE limits. First the baseline data for a given sensor location is analyzed to determine its mean value ($\bar{m}$) and standard deviation (σ). Second the yellow and red limits for the M2 type sensors are calculated as $\bar{m} + 2\sigma$ and $\bar{m} + 3\sigma$ respectively. Assuming a normal distribution of SPADE readings for a population of baseline components of the same type, the probability of a false yellow light is about 2.3%, and the probability of a false red light is about 0.1%.

Next the M3 sensor modification factors were applied to these limits. The first factor takes into account the difference between M2 and M3 type sensors. A sensitivity factor was calculated for each of the ten UH-1H sensor locations by taking the ratio of the spec value for M3 sensor sensitivity to the calibrated sensitivity for the individual M2 sensor used to accumulate the bulk of the baseline data at each sensor location. Thus we have:

$$\text{Transducer Sensitivity Factor} = \frac{\text{M3 Spec. Sensitivity}}{\text{M2 Calib. Sensitivity}} = \text{TSF}$$

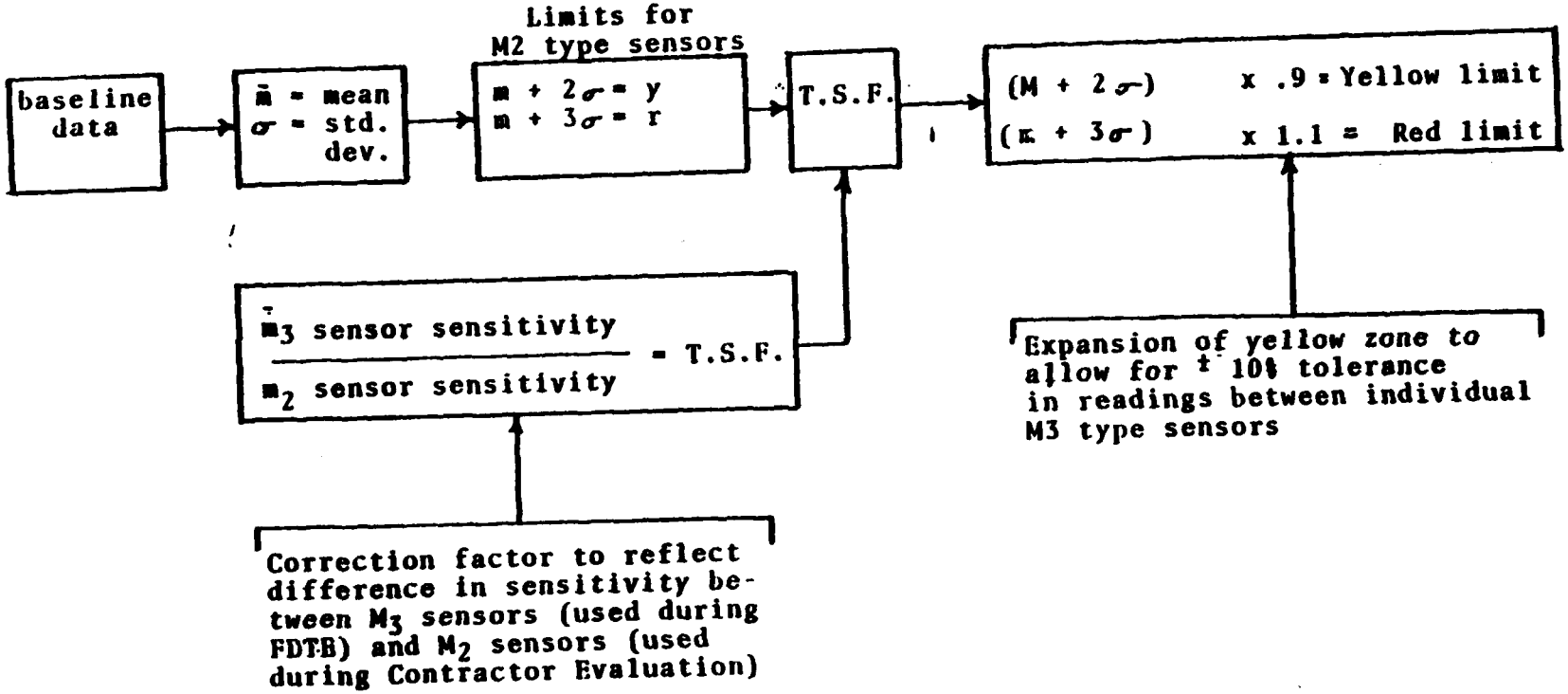

Sample Calculation for Input Pinion Sensor Location:

Baseline Data	Statistical Data		T.S.F.	m_3 Sensor Limit Calculations
Range = 05-37	$\bar{m} = 23.5$ $\sigma = 11.2$	$\bar{m} + 2\sigma = 45.9$ $\bar{m} + 3\sigma = 57.1$	1.32	$1.32\ (\bar{m} + 2\sigma)\ .90 = 54.5$ (yellow) $1.32\ (\bar{m} + 3\sigma)\ 1.10 = 82.9$ (red)

Figure 21
SPADE LIMIT CALCULATIONS

The second modifying factor applied to the M2 limits takes into account the spec-allowable tolerance on M3 sensor-to-sensor sensitivity variations. (This is to allow for interchangeability of sensors in the operational use of SPADE) Since this spec-allowable sensitivity tolerance is ± 10%, the lower limit of the yellow zone (the yellow light threshold) was decreased by 10% and the upper limit of the yellow zone (the red light threshold) was increased by 10%. Figure 21 shows the limit calculations for the Transmission Input Pinion sensor location on the UH-1H.

Table XIV lists the limit values calculated for each sensor location for both the old (M2) sensors and the new (M3) sensors. Since the hanger bearing limits were greater than 100%, it was necessary to divide all values by four (4) and make a corresponding change to the digital circuitry in the Central Processor Unit (CPU). These final programmed limit values are listed in Table XV and shown graphically in Figures 22 and 23 .

4.4 SPADE Accuracy - Estimating the diagnostic accuracy of the SPADE unit at this early stage in its development is uncertain at best. This is primarily due to two factors: the first being the relatively small sample of aircraft used in acquiring baseline data and developing warning limits for the whole population of UH-1H & AH-1G aircraft; and the second factor being the use of "implanted" rather than "naturally occurring" defects to verify the SPADE detection capability. In addition there are other factors which must be considered; such as, SPADE operational philosophy and the failure progression intervals for different failure modes of different bearings.

Sensor Location	SPADE Channel Number	Limit Set #1 (New, M3, Sensors)		Limit Set #2 (Old, M2, Sensors)	
		Yellow	Red	Yellow	Red
Transmission Input Pinion	1	54.5	82.9	41.3	62.8
Transmission Upper Mast Bearing	2	27.8	38.6	20.9	29.
Tail Rotor Drive Quill	3	27.6	40.2	28.2	41.0
42° Gearbox Input	4	17.1	25.6	17.6	26.4
42° Gearbox Output	5	18.5	26.9	17.0	24.6
90° Gearbox	6	10.3	16.0	10.6	16.5
#1 Hanger Bearing	7	201	322	190	304
#2 Hanger Bearing	10	222	366	158	259
#3 Hanger Bearing	8	115	180	108	170
#4 Hanger Bearing	9	172	263	168	258

Table XIV
SPADE UH-1H/AH-1G LIMITS

(Calculated Values)

Sensor Location	SPADE Channel Number	Limit Set #1 (New, M3, Sensors)		Limit Set #2 (Old, M2, Sensors)	
		Yellow	Red	Yellow	Red
Transmission Input Pinion	1	13.6	20.7	10.3	15.7
Transmission Upper Mast Bearing	2	6.9	9.7	5.2	7.3
Tail Rotor Drive Quill	3	6.9	10.1	7.0	10.3
42 Gearbox Input	4	4.3	6.4	4.4	6.6
42 Gearbox Output	5	4.6	6.7	4.2	6.2
90 Gearbox	6	2.6	4.0	2.6	4.1
#1 Hanger Bearing	7	50.2	80.5	47.4	75.9
#2 Hanger Bearing	10	55.5	91.4	39.4	64.8
#3 Hanger Bearing	8	28.7	45.0	27.1	42.4
#4 Hanger Bearing	9	42.9	65.8	42.0	64.6

Table XV
SPADE UH-1H/AH-1G Limits

(Programmed Values)

Figure 22

UH-1H/AH-1G

SPADE LIMIT VALUES

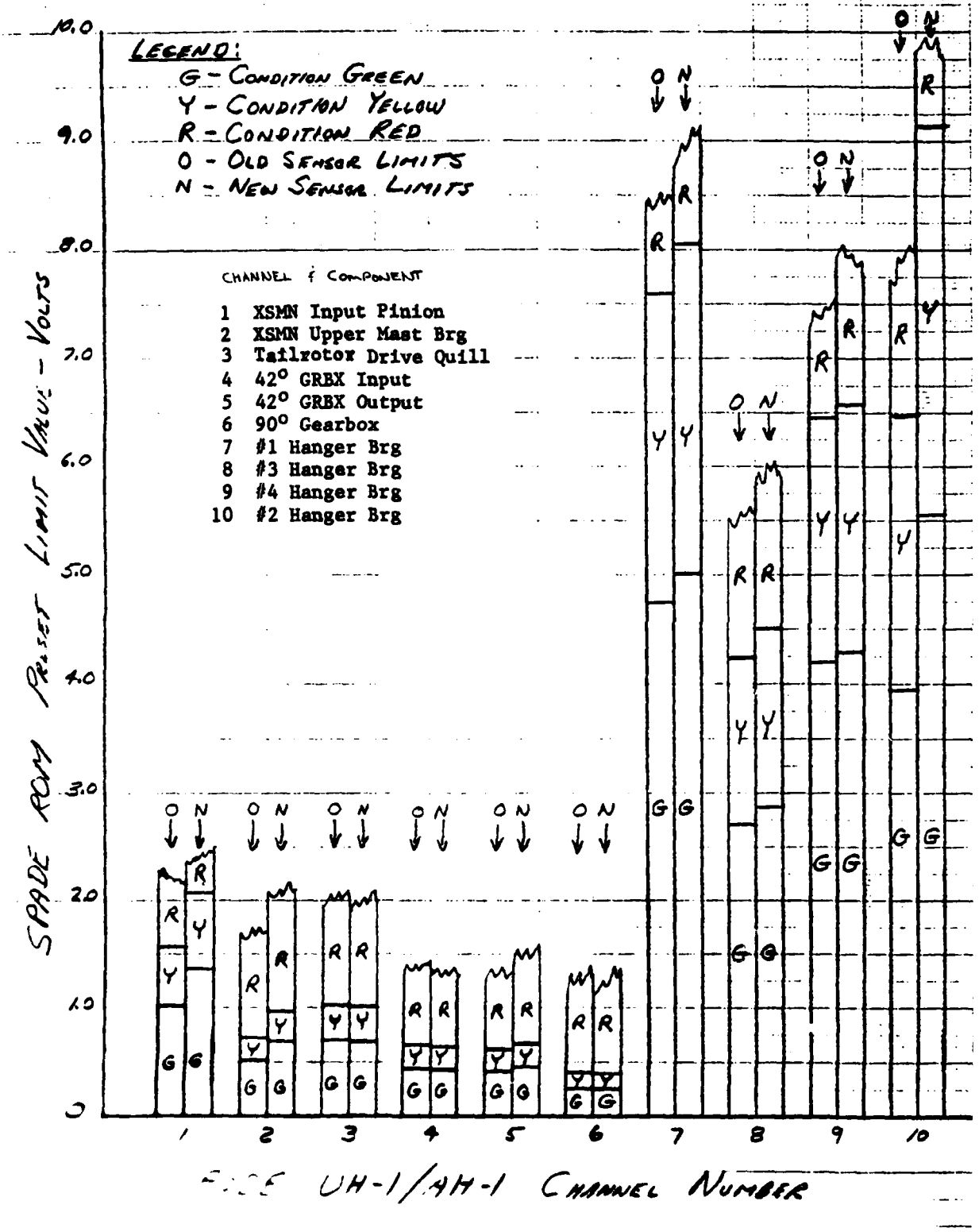

* All limits are expressed as a percentage of SPADE's linear dynamic range.

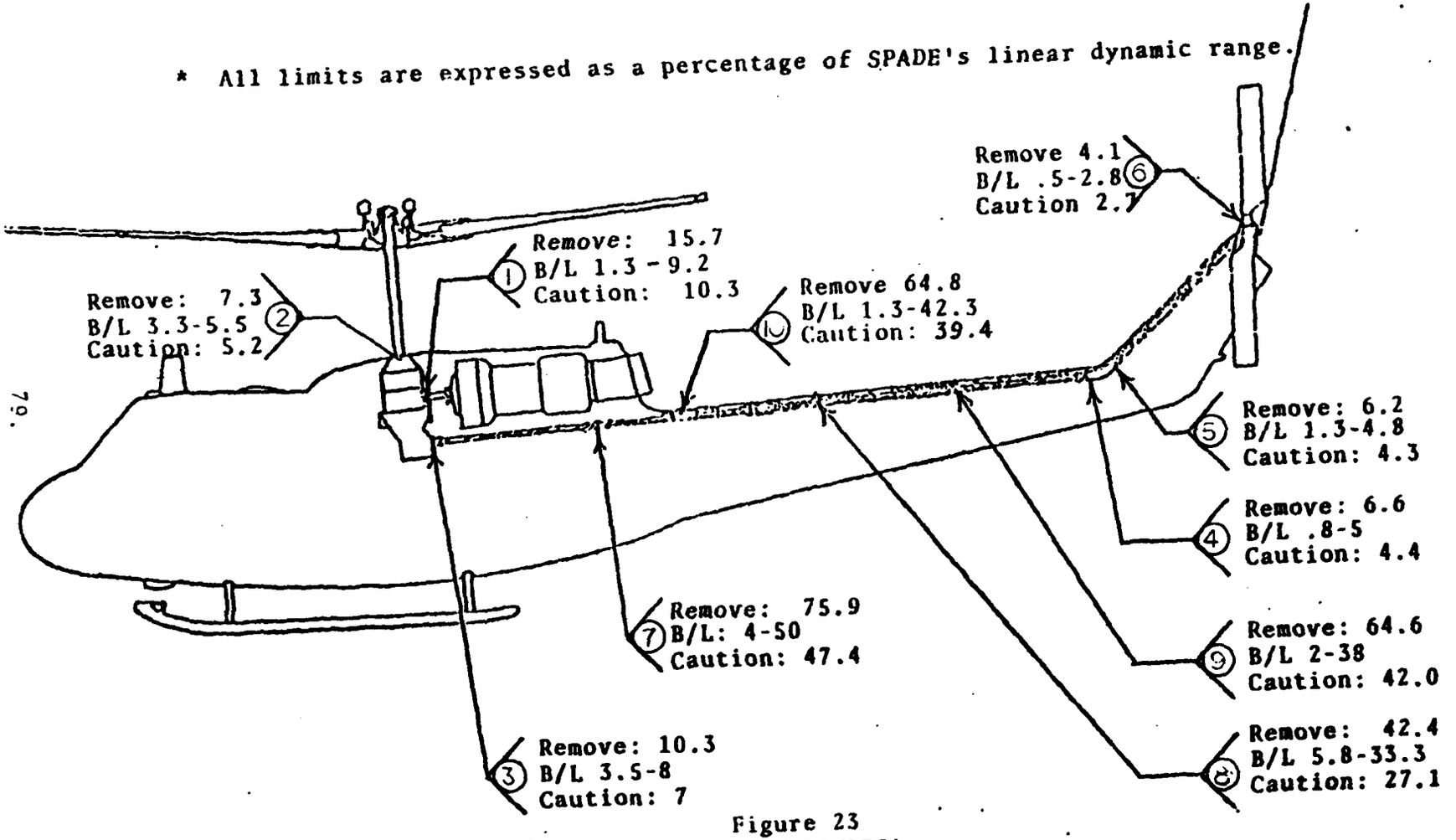

Figure 23
SPADE UH-1H LIMITS*
(M3 Sensors Only)

4.4.1 Contractor Evaluation SPADE Accuracy - Table XVI lists the number of red, yellow, green lights obtained for each implant configuration tested during ground runs on the "Bearcat 14" UH-1H test aircraft. The far right-hand column of this table is the calculated value for the instantaneous (each time a SPADE reading is taken) probability of calling a discrepant part defective. P_{4i}. This instantaneous probability of fault detection is calculated two ways: First, considering only red lights as "HITS", and second, considering both red and yellow lights as "HITS". All green lights are considered "MISSES" and P_{4i} is calculated as the ratio of "HITS" to the total of Hits + MISSES, thus:

$$P_{4i} = \frac{\text{No. of "HITS"}}{\text{HITS + MISSES}} = \frac{\text{No. of "HITS"}}{\text{Total No. of Tests}}$$

These calculated values of instantaneous fault detection probabilities are lower than would be expected in operational use for the following reasons:

1.) The process of implanting a discrepant component into an "alien" gearbox results in decreased levels of kinetic energy due to:

   a.) Misindexing of the defect relative to its natural location in its "native" gearbox.

   b.) Removal of trapped debris generated by the defect.

2.) The above data was, for the most part, accumulated from bearings with defects that were small relative to the levels of damage which would result in loss of load carrying capability for a bearing. Since SPADE read-

Table XVI

SPADE CONTRACTOR EVALUATION

TEST RESULTS

XMSN INPUT PINION

Implant #	No. of Indications Green	Yellow	Red	P^*_{4i} R	P^*_{4i} R + Y
BHC-093			4		
MAIC-025			1		
BHC -012	1				
BHC-081	2				
MAIC-018	2				
TOTALS:	5		5	.50	.50

* P_{4i} = Instantaneous Probability (each time a SPADE reading is taken) of calling a discrepant part defective.

XMSN MAST BEARING

Implant #	No. of Indications Green	Yellow	Red	P_{4i} R	P_{4i} R + Y
SKF-025			2		
BHC-124	2				
BHC-132	2				
TOTALS:	4		2	.33	.33

XMSN TAIL ROTOR DRIVE QUILL

Implant #	No. of Indications Green	Yellow	Red	P_{4i} R	P_{4i} R + Y
BHC-023			2		
BHC-008		2			
MAIC-009	1	1			
TOTALS:	1	3	2	.33	.83

42° GEARBOX INPUT

Implant #	No. of Indications Green	Yellow	Red	P_{4i} R	P_{4i} R + Y
MAIC-009			1		
BHC-001			2		
MAIC-011	2		2		
TOTALS:	2		5	.71	.71

42° GEARBOX OUTPUT

Implant #	No. of Indications Green	Yellow	Red	P_{4i} R	P_{4i} R + Y
BHC-013			1		
MAIC-010			2		
MAIC-001			2		
TOTALS:			5	1.00	1.00

90° GEARBOX

Implant #	No. of Indications Green	Yellow	Red	P_{4i} R	P_{4i} R & Y
BHC-025			2		
BHC-031			5		
MAIC-014	1	1			
BHC-099		2			
BHC-091		2			
TOTALS:	1	5	7	.54	.92

TAIL ROTOR DRIVESHAFT HANGER BEARINGS

Implant #	No. of Indications Green	Yellow	Red	P_{4i} R	P_{4i} R + Y
SKF-003	2				
SKF-002	1	4	7		
SKF-001		1	11		
SKF-024	3	2			
SKF-005	2	1	1		
SKF-023			5		
SKF-004	2				
TOTALS:	10	8	24	.57	.76

CH-1H DRIVE TRAIN TOTALS (excluding engine)

Component	No. of Indications Green	Yellow	Red	P_{4i} R	P_{4i} R + Y
Main transmission	10	3	9	.41	.55
42° Gearbox	2	0	10	.83	.83
90° Gearbox	1	5	7	.54	.92
Hanger Bearings	10	8	24	.57	.76
TOTALS:	23	16	50	.56	.74

ings are proportional to the level of damage within a bearing, higher readings and higher detection rates would result if larger defects were implanted or if those implants that read "yellow" when tested were allowed to progress to more significant levels of damage.

In addition, the above detection probabilities are for each time that a SPADE measurement is taken on a discrepant bearing. However, since bearings do not fail instantaneously, the SPADE can be used several times (on a regularly scheduled basis) between the time an initial discrepancy appears and the time a bearing is so badly damaged that it loses its load carrying capability. This period between initial discrepancy and loss of function for a bearing is called the Failure Progression Interval (I_f). The number of aircraft operating hours between scheduled SPADE inspections is known as the Utilization Interval (U). The cumulative detection probability (P_{4c}) for SPADE is greater than its instantaneous value (P_{4i}) because during the failure progression interval there are several chances (I_f/U) for finding the defect, and only one red light is required to remove the failing component from service. Equation I defines the mathematical relationship between the cumulative probability of detecting an on-going failure and these other diagnostic parameters P_{4i}, I_f, and U.

$$P_{4c} = 1 - (1-P_{4i})^{If/U} \quad \text{Equation 1 (from Ref. 2)}$$

Given this relationship and the experimental values for P_{4i}, it remains to estimate the failure progression interval, I_f, for bearings, and to select a SPADE Utilization Interval (U) that yields a satisfactory cumulative probability of fault detection. Of all the

bearings used for implant testing during this and preceding Army diagnostic test programs, none has shown evidence of significant failure progression. Of these same bearings, eleven have been operated for times in excess of 100 hours and three in excess of 200 hours with a maximum spalled bearing operating time of just over 290 hours. Since no significant damage progression occurred during all this testing, the failure progression interval, I_f, has been conservatively estimated at 200 hours. Figure 24 shows SPADE's cumulative probability of fault detection as a function of its utilization interval. The four curves in this figure represent a range of instantaneous fault detection probabilities which "bracket" the results of testing during the Contractor Evaluation of SPADE. The important message from this figure is that even for the worst case estimate of SPADE accuracy, a cumulative probability of fault detection in excess of 94% can be achieved with a 25 hour SPADE inspection interval. Indeed, a less pessimistic estimate of SPADE accuracy (P_{4i}=.45) would indicate a cumulative probability of fault detection in excess of 99% at a 25 hour inspection interval and better than 90% at a 50 hour interval. In addition, any increase of the failure progression interval above 200 hours will result in an increase in the cumulative probability of fault detection.

The other side of the coin, of course, is the false indication rate that can be expected when employing the same limits that are associated with the detection accuracy just discussed. The yellow and red indication limits in SPADE are set at the mean plus 2-sigma ($\bar{m}$ + 2 ·) and mean plus 3-sigma ($\bar{m}$ + 3 ·) values respectively of all the confirmed baseline data accumulated from UH-1H aircraft during the Contractor Evaluation. Assuming a normal distribution of measure-

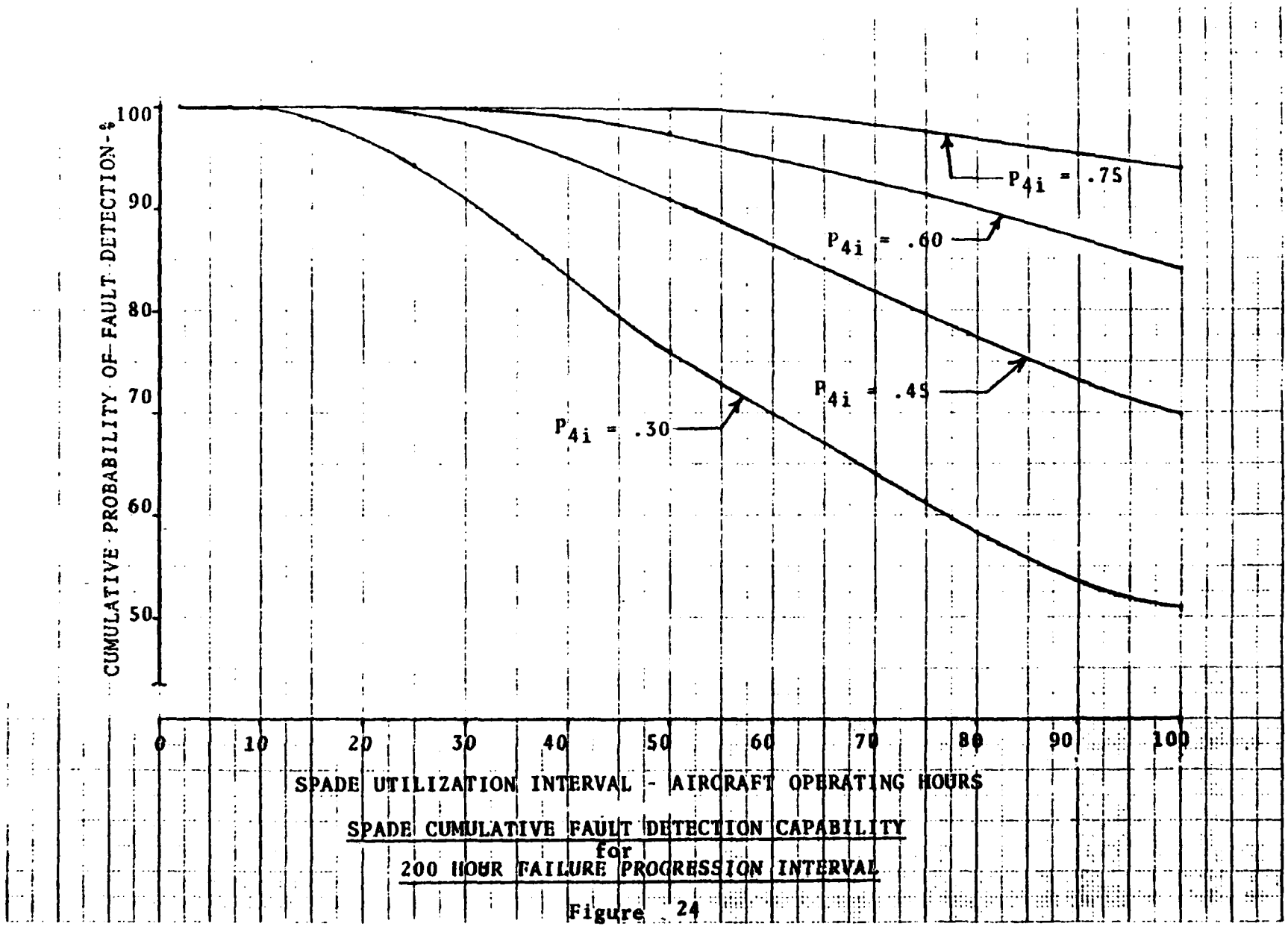

SPADE CUMULATIVE FAULT DETECTION CAPABILITY
for
200 HOUR FAILURE PROGRESSION INTERVAL

Figure 24

ments, this should result in an instantaneous probability of false removal indication (P_{2i}) of .00135. The cumulative probability of false removal indication (P_{2c}) would then be the product of the number of SPADE measurements times P_{2i}. The Mean Time Between Removals due to false indications ($MTBR_{fi}$) for each drive train component monitored by SPADE can be calculated from Equation 2, given below:

$$MIBR_{fi} = \frac{\text{SPADE UTILIZATION INTERVAL}}{\text{No. of sensors on component x } P_{2i}} \quad \text{Equation 2}$$

Table XVII lists the $MTBR_{fi}$ and corresponding false removal rate for each aircraft component at two SPADE Utilization Intervals (U=25 hr & U=50 hr). This table also summarizes false removal rates for the total UH-1H drive train and the gearboxes vs tail rotor driveshaft hanger bearings as separate component classes. It is important to note from this table that even for a 25 flight hour SPADE Utilization Interval, the false removal rate is slightly less than one removal per thousand aircraft flight hours.

In summary then, even a pessimistic assessment of SPADE Contractor Evaluation test results indicates a fault detection capability of 94% and a false removal rate of one per thousand flight hours. This accuracy exceeds the proposed L.R. values of 90% fault detection capability and 2 false removals per thousand flight hours.

4.4.2 SPADE Tolerance - In any measurement system there are certain inaccuracies introduced by the performance tolerances of the system elements. In SPADE these inaccuracies are broken into three categories: sensor tolerances, SPADE Electronic Unit (EU) tolerances, and kinetic/

AIRCRAFT COMPONENT	$MTBR_{fi}$ - Flt. Hr.		False Removals/1000 Flt hr.	
	U* = 25 flt. hr	U* = 50 flt hr	U* = 25 flt hr	U*= 50 flt hr
Main Transmission	6173	12346	.162	.081
42 Gearbox	9259	18518	.108	.054
90 Gearbox	18519	37038	.054	.027
T/R Drive Hanger Bearing	18519	37038	.054	.027
Transmission & Gearboxes	3086	6172	.324	.162
Four (4) Hanger Bearings	4630	9260	.216	.108
TOTAL DRIVETRAIN (Excl. Engine)	1089	2179	.918	.459

*U = SPADE UTILIZATION INTERVAL

TABLE XVII

SPADE CAUSED FALSE REMOVAL RATES

frictional energy fluctuations. The sensor tolerance refers to the range of readings that may be obtained from a common input due to sensitivity variations between interchangeable sensors. The EU tolerance refers to the range of readings that may be obtained due to hysteresis within the SPADE signal conditioning and data processing circuitry. Kinetic and frictional energy fluctuations take into account the fact that no real machine operates at an absolutely steady-state level of efficiency and corresponding kinetic/frictional energy losses. These three basic factors interact with one another in a random fashion to sometimes increase, and sometimes decrease, the total amount of uncertainty inherent in any SPADE measurement. To express this mathematically we say:

$$\begin{matrix}\text{Total SPADE} \\ \text{Tolerance}\end{matrix} = \begin{matrix}\text{Kinetic/Frictional} \\ \text{Energy Fluctuation}\end{matrix} \times \begin{matrix}\text{Sensor} \\ \text{Tolerance}\end{matrix} \times \begin{matrix}\text{Electronic Unit} \\ \text{Tolerance}\end{matrix}$$

$$= K \cdot S \cdot E$$

where K = Kinetic Energy Fluctuation

S = Sensor Tolerance

E = Electronic Unit Tolerance

The Electronic Unit Tolerance, E, is about $\pm$ 1% at the median value of its range. This can be demonstrated by operating the unit in the SELF TEST mode and observing the range of values shown in the PERCENT display. Therefore:

$$E = 1.01$$

The effect of normal kinetic (and frictional) energy fluctuations within a grease lubricated ball bearing can be approximated by examination of the variation in readings taken by one sensor (AA01-

M3) over a two day period of intermittant operation, from bearing 1-B of the Bearing Test Fixture (BTF). The readings ranged from 17 to 24 (median = 20.5) so the fluctuation is ± 17%. Therefore:

$$K = 1.17$$

The combined tolerance due to both the SPADE Electronic Unit Hysteresis and kinetic/frictional energy fluctuations can then be approximated as:

$$\begin{matrix}\text{SPADE Tolerance} \\ \text{(excluding sensor effects)}\end{matrix} = E_1 K = 1.01 \times 1.17 = 1.18$$

Thus SPADE readings should be accurate to within ± 18% of their "true" value if the effect of interchangeable sensors is eliminated. Although this tolerance estimate was derived from laboratory test data, it is reasonably well confirmed by the Contractor Evaluation on-aircraft test data in Table XVIII. This data was taken with two SPADE Electronic Units but with no change in sensors on each of two different aircraft. The overall average tolerance due to kinetic/frictional energy fluctuations and Electronic Unit Hysteresis was ± 13% as opposed to the ± 18% laboratory value.

The total SPADE tolerance (including that due to interchangeable sensors) can be estimated from data accumulated over a two day period by all forty (40) of the model M3 sensors on bearing 1-B of the BTF. The readings ranged from 12 to 26 (median = 19) so the SPADE total tolerance is ± 37%. Thus we have:

$$1.37 = 1.17 \times \begin{matrix}\text{Sensor} \\ \text{Tolerance}\end{matrix} \times 1.01$$

$$\begin{matrix}\text{Sensor} \\ \text{Tolerance}\end{matrix} = \frac{1.37}{1.17 \times 1.01} = 1.159 \text{ thus } S = 1.16$$

Thus due to sensitivity differences between sensors, SPADE readings can fluctuate by ± 16% of the median value. Since this

TABLE XVIII

SPADE Tolerance (Excluding Sensor Effects)

SPADE SENSOR LOCATION	RUN 65-B BEARCAT - 13				RUN 67-B BEARCAT - 14				Both Aircraft
	SPADE 001	SPADE 002	BC-13 Median	Max.% Dev.	SPADE 001	SPADE 002	BC-14 Median	Max.% Dev.	Avg.% Max. Dev.
Xmsn. Mast	N/A	N/A	--	--	13-14	14-16	14.5	± 10%	± 10%
Xmsn. I.P.	05-06	06	5.5	± 9%	25-26	34	29.5	± 15%	± 12%
Xmsn. T.R.	12-13	12-13	12.5	± 4%	21-22	22-23	22	± 5%	± 5%
#1 H.B.	17	16-18	17	± 6%	B/L ?	B/L ?	--	--	± 6%
#2 H.B.	88-107	123-127	107.5	± 18%	B/L ?	B/L ?	--	--	± 18%
#3 H.B.	B/L ?	B/L ?	---	---	23-25	30-39	31	± 26%	± 26%
#4 H.B.	08-11	07	9	± 22%	B/L ?	B/L ?	---	---	± 22%
42° I.P.	03	03-04	3.5	± 14%	12-13	12-13	12-5	± 4%	± 9%
42° O.P.	08-09	09-11	9.5	± 16%	12	11-12	11-5	± 4%	± 10%
90° G.B.	11	08-10	9.5	± 16%	09-11	10-11	10	± 10%	± 13%
Total aircraft Avg. Dev. %				± 13%				± 11%	± 13%

value for sensor tolerance is greater than the ± 10% called out in the M3 sensor specification, it implies the need for recalculating limit thresholds to prevent the possibility of getting widely divergent readings when using sensors on an interchangeable basis.

In setting limits into SPADE memory, two criteria must be met:

1.) The false red light alarm rate must be minimized, and

2.) Red light alarms must not be ambiguous.

To satisfy the above criteria, a yellow caution zone must be defined that takes into account a worst case build-up of SPADE tolerance effects. This means that the mid-point of the yellow zone must be high enough to allow for a ±40% tolerance band without falling below the yellow limit or rising above the red limit. These are boundary conditions that can be expressed mathematically as follows:

Let R = Red limit threshold

Let Y = Yellow limit threshold

Let Z = Median value of the yellow zone

The yellow zone median can then be expressed in terms of the Red and Yellow limit thresholds as:

$$Z = \frac{R - Y}{2} + Y \qquad \text{Equation 3}$$

Now to allow for a ± 40% tolerance and express Z as a function of Y we define:

$$Y = .6Z$$

$$Z = 1.7Y \qquad \text{Equation 4}$$

AD-A083 652 SKF INDUSTRIES INC KING OF PRUSSIA PA F/G 1/3
SMALL PORTABLE ANALYZER DIAGNOSTIC EQUIPMENT (SPADE) - ADVANCE --ETC(U)
SEP 79 D B BOARD DAAJ01-76-C-1073
UNCLASSIFIED SKF-AL99Q016 USAAVRADCOM-TR-80-F-3 NL

2 : 2

END
DATE FILMED
6 80
DTIC

And by substituting Equation 4 into Equation 3 we get:

$$1.7\ Y = \frac{R - Y}{2} + Y$$

$$.7\ Y = \frac{R - Y}{2}$$

$$1.4\ Y = R - Y$$

$$2.4\ Y = R \qquad \text{Equation 5}$$

Thus Equation 5 defines the minimum allowable value for a red limit that will not result in ambiguous indications when the SPADE tolerance is as high as $\pm$ 40%. The yellow limit value, Y, is defined as the mean plus 2-sigma ($\bar{m} + 2\sigma$) value of baseline data to assure a low probability of false alarm.(See Section 4.3).

Figure 25 illustrates the above relationships graphically. Three cases are shown for a hypothetical sensor location. In Case 1, the yellow zone is defined according to Equation 5; in Case 2 the yellow zone is smaller than in Case 1; and in Case 3 the yellow zone is larger than in Case 1. From this figure it is apparent that in Case 1 ambiguous indications ranging from green to red are not possible but that in Case 2 either a green or red light could be obtained from a component with a true value at the mid-point of the yellow zone depending upon the build-up of tolerances from interchangeable sensors and transient fluctuations of kinetic/frictional energy. In Case 3 ambiguous indications are not a problem,but since the red limit is higher the defect cannot be found as early in its failure progression. This has the effect of decreasing the failure progression interval, I_f, and thus reducing the cumulative probability of fault detection (refer to Equation 1).

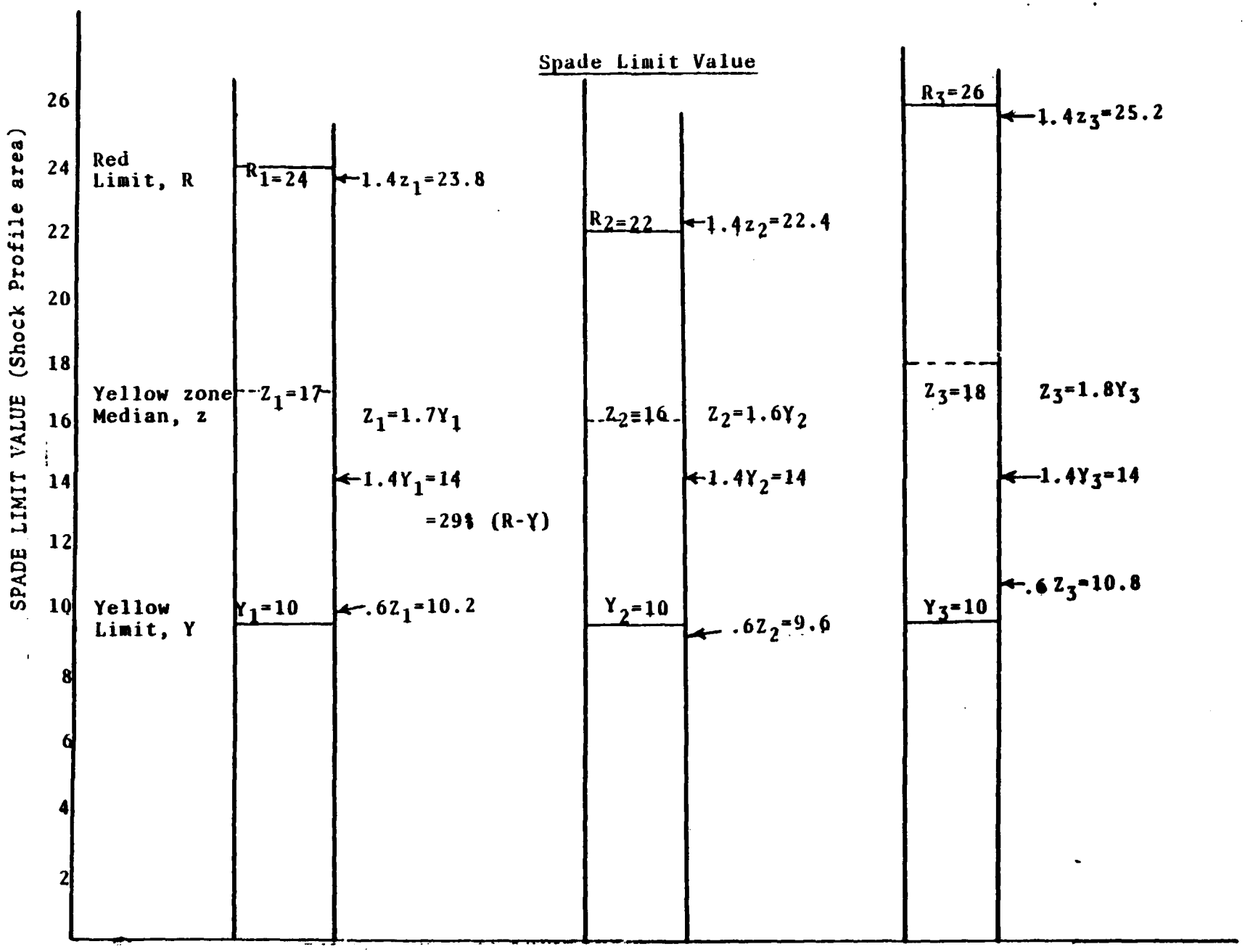

FIGURE 25 - RELATIONSHIP OF SPADE TOLERANCE TO YELLOW ZONE

Case 1 of Figure 25 also points out that for a baseline (undamaged) component that normally reads in the high end of the green zone, the maximum PERCENT DEGRADATION value to be expected from tolerance build-up is 29%. Therefore, it is recommended that only components which read greater than 29% into the yellow zone should be trended for predictive maintenance purposes.

A few final remarks relative to this method of setting red limit thresholds are appropriate here. Along with the previously stated criteria for non-ambiguous indications and a low false alarm rate, there is also a requirement that the red limit must not be set so high that significant defects are not detectable in a timely manner. By the method defined in Equation 5, the red limit is always less than 2.5 times the maximum value of baseline components. Thus defective components that are sufficiently degraded to warrant removal should read at least 2.5 times the yellow limit value. This is not an unreasonable expectation for SPADE since it measures total energy as a function of both the amplitude and frequency of shock pulses generated by kinetic and frictional events within a machine. It has repeatedly been shown during this and other programs that even small artificially implanted defects cause shock pulse amplitudes to increase by a factor of more than 3 to 1 (10db). In addition, the rate at which shock pulses are generated by discrepant bearings rises dramatically as a function of defect size. This is substantiated by the fact that during the Contractor Evaluation implant testing one or more of the implant conditions tested at every sensor location produced readings in excess of 2.5 times the ($\bar{m}+2\sigma$) yellow limit.

5.0 Low Cost Sensor Development & Evaluation - The Endevco and B & K sensors (both M2 and M3 types) that were used with SPADE during the Contractor Evaluation and the FDTE were modifications of standard low frequency accelerometers. However, since the low frequency response of these sensors is filtered out for shock pulse analysis, only the resonant output is significant. A good deal of the cost associated with the manufacture of accelerometers is related to assuring flat response (constant sensitivity as a function of frequency) below resonance. It was therefore decided to try to develop a lower cost piezoelectric sensor with response characteristics specified for resonant output only. To this end, several vendors were contacted and BBN Instruments Co. was selected to build a small quantity of sensors with a target cost of $50 each in quantities of 500 or more. Table XIX lists the specification parameters and values defined for these "Low Cost" sensors.

5.1 On-Aircraft Testing - As pointed out in section 4 on the Contractor Evaluation, these sensors were found to be unacceptable during both baseline and implant testing on the UH-1 aircraft at Ft. Rucker. The problem was that the SPADE readings obtained from the same sensor location varied quite widely, apparently due to large differences in resonant sensitivity from one low cost sensor to another. Thus the on-aircraft data obtained from BBN sensors was unsuitable for calculating limits and a laboratory investigation was initiated to define the cause of the unacceptably high sensor-to-sensor resonant sensitivity variations.

5.2 Laboratory Testing - Figure 26 shows the test set-up employed for the laboratory investigation of the BBN sensor problem. A

Table XIX

Original Specification
for
Low Cost Shock Pulse Sensor

1.	Voltage Sensitivity at Resonance	170 mv/g ± 10%
2.	Operating Temperature Range	-10°C to 100°C
3.	Operating Range	0 to 5000 g's
4.	Shock Survivability (peak g's)	5000 g's
5.	Frequency Response	at least 30 db peak factor at resonance
6.	Mounted Resonant Frequency	40 KHz ± 3KHz
7.	Grounding	case
8.	Connector:	
	Accelerometer	BNC female
	Mating	BNC male
9.	Weight	20 grams or less
10.	Size	.625 diam. or less
11.	Mounting	10-32 female, .19" deep minimum

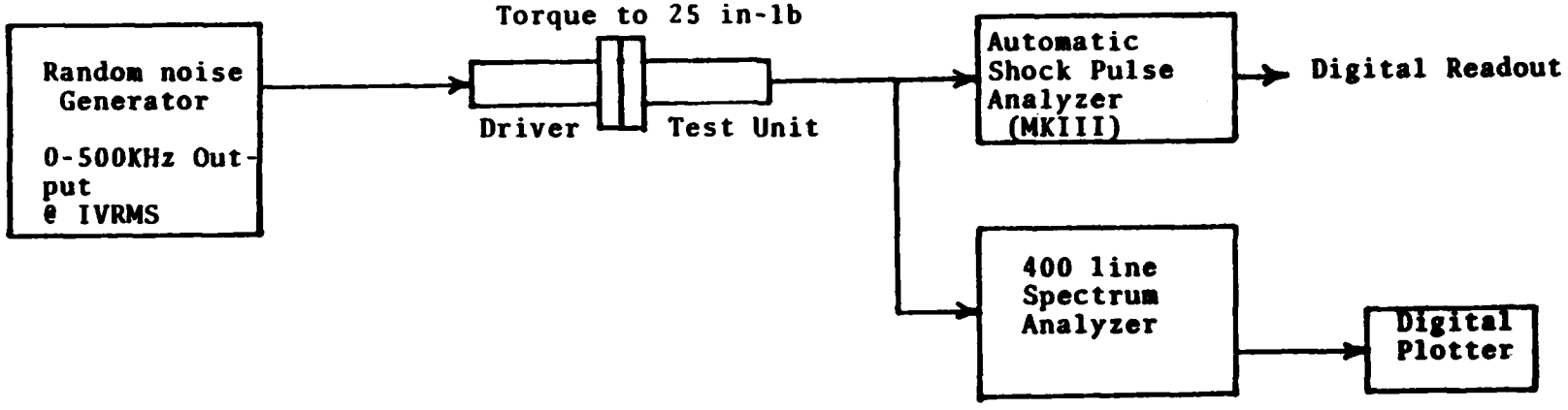

FIGURE 26 - BBN SENSOR, LABORATORY TEST SET-UP

Random Noise Generator (RNG) with a 0-500KHz output at 1 volt RMS was used to excite an Endevco 6224 (M2 type) sensor which served as a standard "driver" to excite each of the BBN Low Cost Sensors. The output from each BBN sensor was then measured in two ways:

1.) The sensor output was processed by a company owned shock pulse analyzer with a 40KHz band-pass filter characteristic identical to those of the SPADE IAPG.

2.) The sensor output was spectrum analyzed to determine the high frequency resonant output as a function of 2 KHz wide frequency bands between 36 KHz and 44 KHz.

Table XX lists the Shock Pulse Analyzer digital readouts obtained during two successive test runs on each of the nine (9) BBN sensors. Each individual reading is the average of 5 measurements. The overall mean value of all 18 readings taken on the 9 sensors was 909. The third and fourth data columns of Table XX show the % deviation from this overall mean for each BBN sensor during Run #1 and Run #2. This data shows that only three (3) of the nine (9) BBN sensors read within $\pm$ 10% of the mean and that individual sensors read as much as 30% above or 33% below the overall mean value for the nine sensors. The last column of this table shows the % variations in readings from Run #1 to Run #2. This data shows that despite dismounting and remounting of each individual sensor, all the sensors read within $\pm$4% of the median value for the two test runs. This means that the majority of the sensor-to-sensor deviation is not due to peculiarities of sensor mounting, but must be due to inherent resonant response

TABLE XX

BBN SENSOR READINGS FROM THE MkIII AUTOMATIC SHOCK PULSE ANALYZER (ASPA)

Sensor Ser. No.	ASPA MkIII Digital Readout Run #1*	Run #2*	%Deviation from Overall Mean Run #1	Run #2	%Variation from Median of 2 Runs
0047	676	726	-26%	-20%	± 4%
0036	617	605	-32%	-33%	± 1%
0034	717	676	-21%	-26%	± 3%
0035	918	912	+ 1%	0%	± 0%
0033	984	973	+ 8%	+ 7%	± 1%
0037	914	903	+ 1%	- 1%	± 1%
0039	1094	1058	+20%	+16%	± 2%
0031	1152	1115	+27%	+23%	± 2%
0041	1119	1184	+23%	+30%	± 3%

Overall mean for the 18 readings above = 909

* Sensors were tested sequentially in two successive test runs. Each reading is the average value of 5 data points.

differences between individual sensors.

Table XXI is a summary of the high frequency energy output by 2 KHz wide frequency bands between 36KHz and 44KHz for each of the BBN sensors. This table shows that all the BBN sensors that gave shock pulse analyzer readings within ±10% of overall mean, also had 36KHz to 44KHz RMS values within ±10% of the overall mean value for 36-44 KHz RMS. However, it is also important to note that while an individual sensor may have an overall 36-44KHz output within ±10% of the mean, it may also have one or more 2 KHz wide bands in the 36-44KHz range that are outside the desired ±10% tolerance for sensor sensitivity. This data implies that there is more than one resonant frequency within the 36KHz to 44KHz frequency range. This observation is substantiated by comparison of the spectral plots in Figure 27. This comparison of the spectral responses of an Endevco 6224-M3 sensor and a BBN sensor shows that while the Endevco sensor has only one major resonance within ±20KHz of the SPADE band-pass filter center frequency of 40 KHz, the BBN sensor has several resonant frequencies. These other resonant frequencies were neither amplitude controlled nor prohibited under the original low-cost sensor specification, but the amplitude variation and degree of interaction varies considerably from one BBN sensor to another as shown in Table XX.

For this reason, a revision, which prohibits any secondary resonance greater than 10 db between 20 KHz and 60 KHz, has been made to the original low cost sensor specification. This revised specification also defines an acceptance test procedure similar to the method described herein for the BBN sensor laboratory testing. This revised

TABLE XXI - BBN SENSOR HIGH FREQUENCY RESONANT OUTPUT BY FREQUENCY BAND

Sensor S/N (2)	Energy in Frequency Band (1) - MV, RMS							
	36-38KHz	38-40KHz	40-42KHz	42-44KHz	36-40KHz	40-44KHz	36-44KHz (3)	0-100KHz
0034 (L)	3.51 *	8.66 (L)	4.08 (L)	4.59 (L)	6.61 (L)	4.34 (L)	5.59 (L)	18.9 *
0036 (L)	3.31 *	7.99 (L)	3.70 (L)	3.05 (L)	6.12 (L)	3.39 (L)	4.95 (L)	17.5 (L)
0047 (L)	1.88 (L)	8.54 (L)	6.51 *	3.60 (L)	6.18 (L)	5.26 (L)	5.74 (L)	17.5 (L)
0033 *	3.11 *	9.00 (L)	6.50 *	6.11 *	6.73 (L)	6.31 *	6.53 *	21.3 *
0035 *	4.11 (H)	9.79 *	5.99 *	8.30 (H)	7.51 *	7.24 (H)	7.38 *	18.6 *
0037 *	3.96 (H)	12.5 (H)	6.33 *	4.73 (L)	9.27 (H)	5.59 *	7.66 *	20.6 *
0031 (H)	2.67 (L)	13.1 (H)	7.96 (H)	6.24 *	9.45 (H)	7.15 (H)	8.38 (H)	23.4 (H)
0039 (H)	4.19 (H)	12.7 (H)	5.73 *	6.92 (H)	9.46 (H)	6.35 *	8.06 (H)	17.3 (L)
0041 (H)	3.56 *	12.6 (H)	7.81 (H)	8.85 (H)	9.26 (H)	8.35 (H)	8.82 (H)	22.3 (H)
$\bar{m}$ - 10%	3.03	9.49	5.46	5.24	7.06	5.40	6.31	17.7
mean (m)	3.37	10.54	6.07	5.82	7.84	6.00	7.01	19.7
$\bar{m}$ + 10%	3.70	11.60	6.67	6.40	8.63	6.60	7.71	21.7

Notes:

(1) Measured by Nicolet 444 Spect. Anal. with 2KHz wide frequency expansion plug-in.

(2) (L) = more than 10% below mean value for these 9 sensors; (H) = more than 10% above mean; * = within ±10% of mean value.

(3) Note perfect correlation with which sensors gave (H), *, and (L) SPA readings.

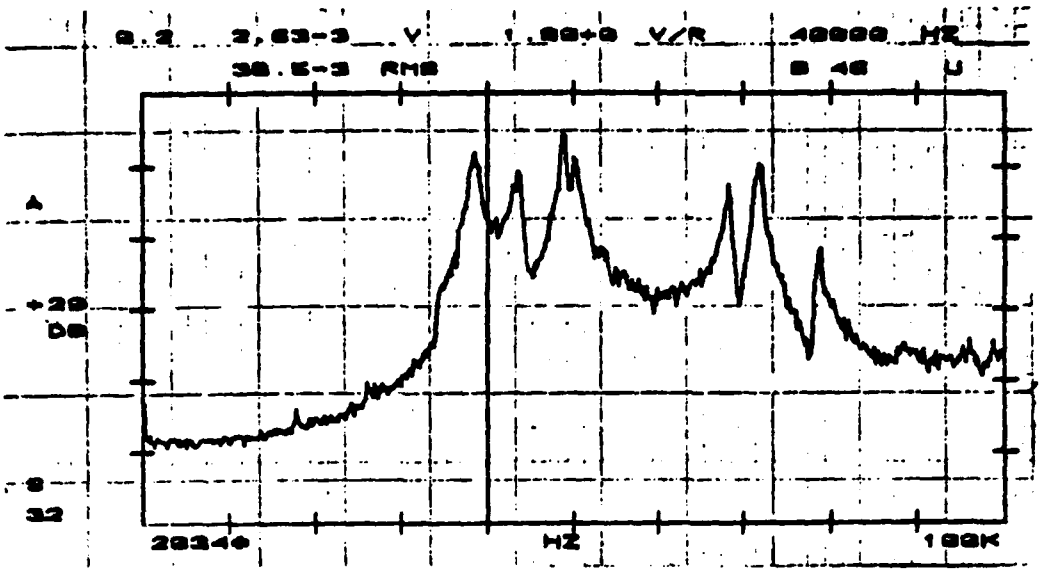

BBN SENSOR NO. 0034

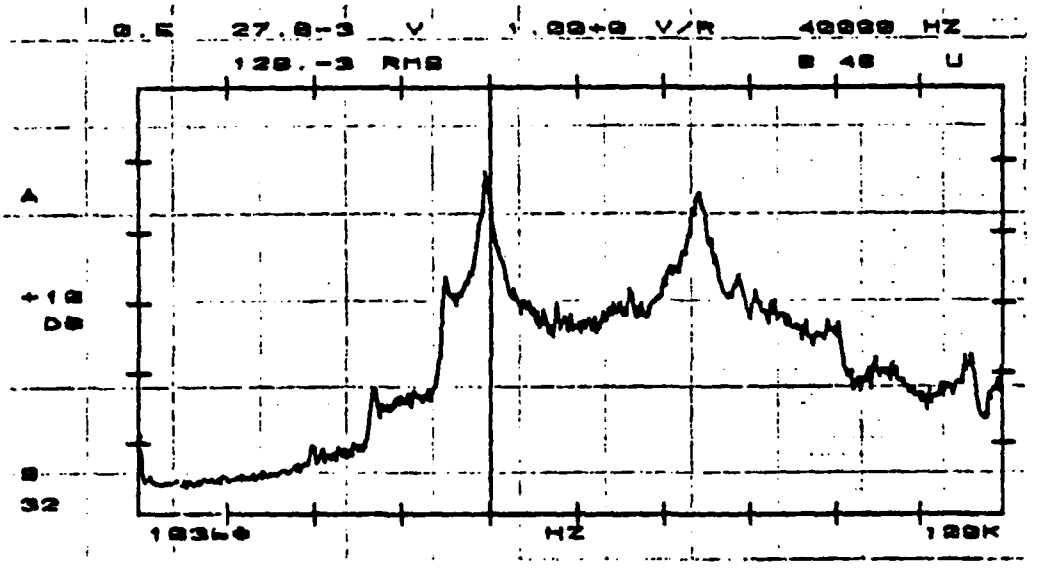

ENDEVCO SENSOR NO. 36

FIGURE 27

TYPICAL FREQUENCY RESPONSE OF ENDEVCO AND BBN SENSORS

specification is shown in Figure 28 and the spectral response of the band-pass filter to be employed for sensor acceptance testing is shown in Figure 29.

Figure 28

SHOCK PULSE SENSOR SPECIFICATION

a.)	Voltage Sensitivity (at resonance)	.81 to .99 Volts (RMS) output from SKF supplied 40 KHZ BPF when driven as shown in the acceptance test procedure of Note A.
b.)	Mounted Resonant Frequency	40 KH_z ± 2 KH_z
c.)	Frequency Response	At least 30 dB peak factor at resonance*
d.)	Operating Temperature Rage	-10 C to 100 C
e.)	Operating Range	0 - 5,000 g's
f.)	Shock Survivability (peak g's)	5,000 g's
g.)	Grounding	Case
h.)	Cable	RG-62 A/U (15 pf/Ft.)
i.)	Connector: accelerometer mating	BNC Female BNC Male
j.)	Weight	20 grams or less
k.)	Size	.625 dia. or less
l.)	Mounting	10-32 female, .19 deep minimum

Note A: Shock Pulse Sensor Acceptance Test Procedure

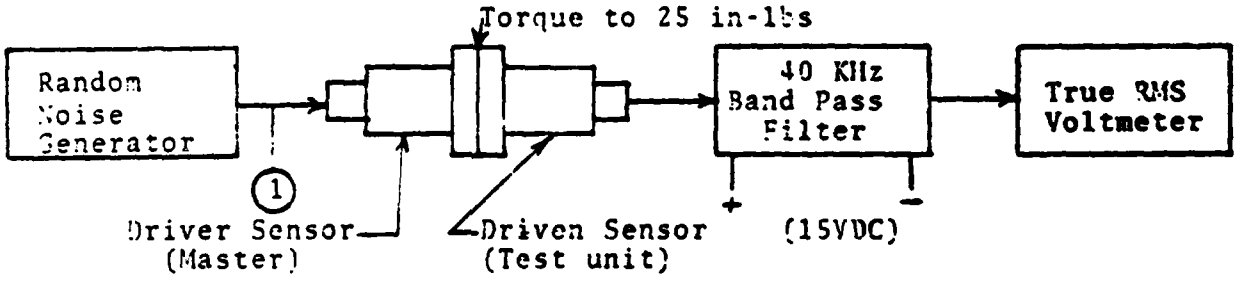

(1) 0-500 KHz Output @ 0.95 V (RMS)

* No additional resonance with a peak factor > 10db is permitted between 20 KH_z and 60 KH_z.

SKF INDUSTRIES, INC. PHILADELPHIA, PA.		DRAWN	CHECK	APPR.	SCALE
					DATE

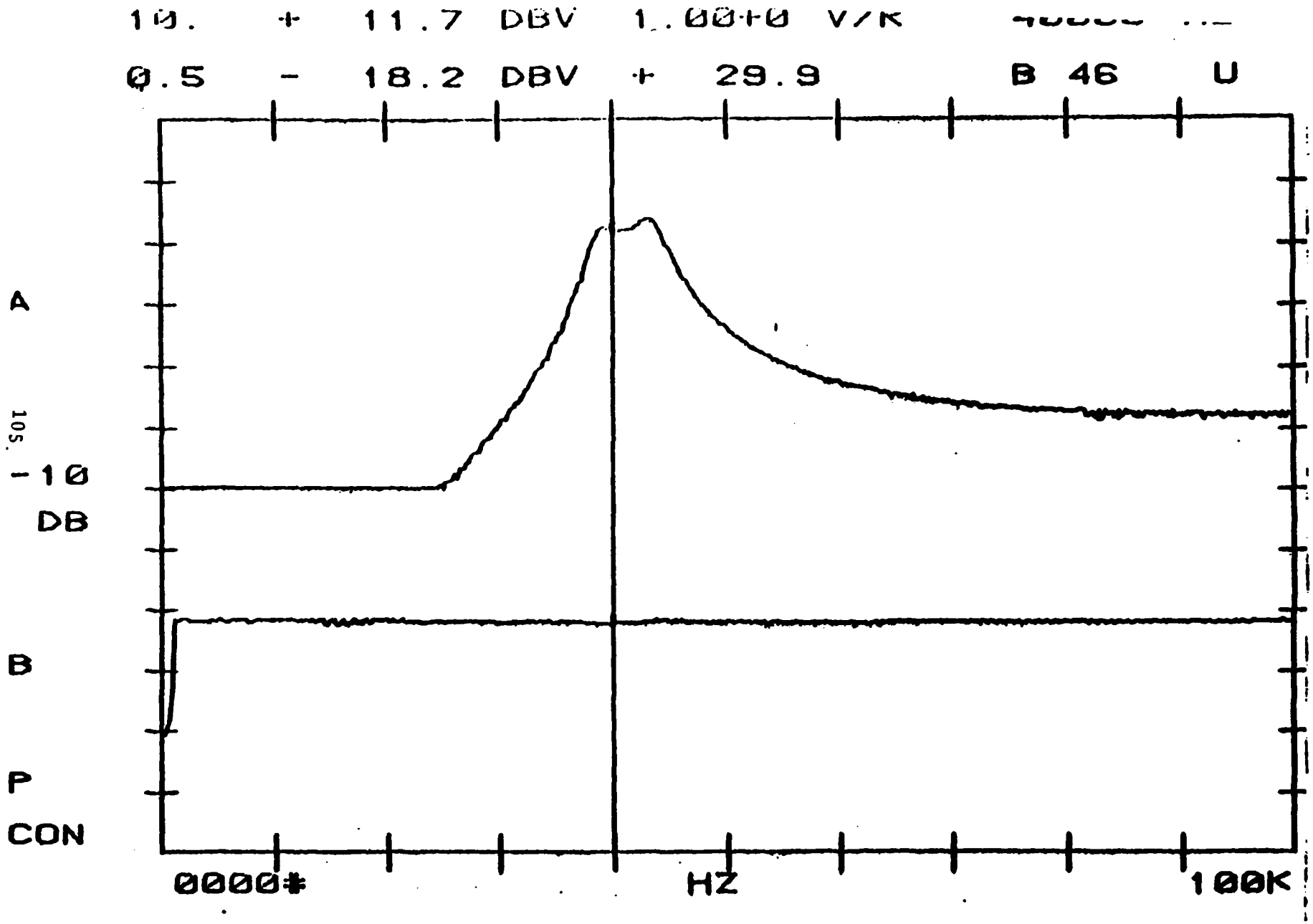

FIGURE 29 - BAND PASS FILTER RESPONSE FOR SENSOR ACCEPTANCE TESTING

6.0 Conclusions and Recommendations

6.1 Conclusions

6.1.1 The SPADE Field Prototypes have been successful in demonstrating the utility, simplicity of operation, durability, and diagnostic accuracy of SPADE. They have also pointed out the need for repackaging to improve portability and for permitting SPADE to operate from 28VDC aircraft power in addition to its own rechargeable battery pack. In addition, several Printed Circuit Boards (PCB's) should be redesigned to incorporate the circuit design refinements that were "jump wired" into the SPADE Electronic Unit during Contractor Evaluation.

6.1.2 Artificial implantation of defective bearings into "alien" drive train components may not produce levels of kinetic impact and frictional energy representative of these same defects in their "native" (where they became discrepant) environment. It is also believed that the implantation process can only tend to decrease SPADE readings relative to those that would be obtained from a "natural" defect in its native environment. These artifically depressed levels of kinetic and frictional energy are probably due to:

a.) misindexing of the surface damage relative to its natural location near the center of the bearing's load zone in its native gearbox; and

b.) removal of particulate debris normally generated by the defect and trapped within the bearing.

6.1.3 Some of the Shock Pulse sensors developed for use in this program did not fully meet the intent of the initial specification issued for their procurement. This resulted in higher than anticipated sensor to sensor variations of resonant sensitivity due to multiple resonances in the 36KHz to 44 KHz frequency band (where only a single, sharp, resonance is desired). The problem was most pronounced in the BBN sensors although the Endevco sensors also suffered the same shortcoming but to a lesser degree. The revised Shock Pulse Sensor procurement specification and acceptance test procedure corrects the initial specification's shortcomings and has been used successfully to procure sensors for a commercial shock pulse analyzer.

6.1.4 The current data base upon which SPADE warning limits and performance characteristics are based is very small (only five Test Board aircraft during Contractor Evaluation). Although the initial test results have indicated that SPADE performs its intended function very well, the warning limits for an aircraft fleet should be determined by quantitative SPADE data on a larger sample of aircraft in different operating environments. In addition, the testing and evaluation conducted to date has not provided a sufficient data base to make quantitative estimates of SPADE's prognostic capability (how SPADE readings change as a function of the level of damage or "remaining safe life" of a discrepant bearing). This type of information is key to determining the optimum utilization interval and operational philosophy for cost effective employment of SPADE in the army aviation environment.

6.2 Recommendations

6.2.1 A SPADE Production Prototype program should be initiated to:

a.) Redesign packaging for improved portability.

b.) Finalize printed circuit board layout and design

c.) Add capability for SPADE to operate from 28 VDC power or its own battery pack (A smaller battery pack than is now used).

d.) Fabricate four (4) Production Prototype SPADE units for use in acquiring additional baseline data, an R & M data base, and definition of prognostic as well as additional (non-bearing) diagnostic applications.

6.2.2 A baseline data collection program should be continued to refine sensor locations and further define alarm thresholds for the following aircraft drive systems: UH-60, CH-47, YAH-64, AH-1, UH-1, OH-58, and OH-6. This data collection effort should include teardown inspection of components identified as suspect from analysis of SPADE data and documentation of SPADE Production Prototype reliability and maintainability characteristics. It is suggested that one or more of the Production Prototypes should be widely circulated to different operating units in diverse environments and that these units be asked to comment upon the relative merits of employing SPADE as a scheduled inspection technique vs. as an unscheduled trouble shooting aid. It is also recommended that warning threshold limits defined under this effort consider the effects of SPADE tolerance as outlined in section 4.4.2 of this report.

6.2.3 An expanded testing program should be initiated to define SPADE prognostic capabilities as well as non-bearing diagnostic applications. Selected discrepant specimens found during the baseline data expansion recommended in 6.2.2, should be run to failure in a test stand while accumulating quantitive SPADE data. These components selected for destructive testing should not be disassembled until after failure, to preclude any uncertainties similar to those involved in implant testing (as discussed in section 6.1.2). SPADE readings accumulated during this type of testing should be trended to establish SPADE's advance warning time as a function of the rate of failure progression in bearings. The data on bearing failure progression and corresponding SPADE readings, along with alarm thresholds determined from baseline aircraft components, should then be used to estimate SPADE's accuracy and cost effectiveness under different operational scenarios.

Definition of expanded diagnostic applications for SPADE should concentrate first on the detection of gear damage, second on the diagnosis of defects in rotating components of turboshaft engines, and third on monitoring hydraulic system components for internal leakage, cavitation, and pump bearing damage.

REFERENCES

1. Spiral Bevel Gear Fault Detection Program; USAAVSCOM; D210-11071-1; Contract DAAJO1-73-A-0017, D0-16.

2. Assessment of Diagnostic/Inspection Technique Interfaces; USAAMRDL: D210-10966-1; Contract DAAJ02-74-C-0030.

3. Transmission Condition Assessment Program; USAAMRDL-TR-76-36; Contract DAAJO2-75-C-0021.